National Library of Canada

Acquisitions and Bibliographic Services Branch

395 Wellington Street
Ottawa, Ontario
K1A 0N4

Bibliothèque nationale du Canada

Direction des acquisitions et des services bibliographiques

395, rue Wellington
Ottawa (Ontario)
K1A 0N4

Your file Votre référence

Our file Notre référence

NOTICE

The quality of this microform is heavily dependent upon the quality of the original thesis submitted for microfilming. Every effort has been made to ensure the highest quality of reproduction possible.

If pages are missing, contact the university which granted the degree.

Some pages may have indistinct print especially if the original pages were typed with a poor typewriter ribbon or if the university sent us an inferior photocopy.

Reproduction in full or in part of this microform is governed by the Canadian Copyright Act, R.S.C. 1970, c. C-30, and subsequent amendments.

AVIS

La qualité de cette microforme dépend grandement de la qualité de la thèse soumise au microfilmage. Nous avons tout fait pour assurer une qualité supérieure de reproduction.

S'il manque des pages, veuillez communiquer avec l'université qui a conféré le grade.

La qualité d'impression de certaines pages peut laisser à désirer, surtout si les pages originales ont été dactylographiées à l'aide d'un ruban usé ou si l'université nous a fait parvenir une photocopie de qualité inférieure.

La reproduction, même partielle, de cette microforme est soumise à la Loi canadienne sur le droit d'auteur, SRC 1970, c. C-30, et ses amendements subséquents.

Canada

University of Alberta

Mechanisms of Nonlinear Pharmacokinetics of Mibefradil

by

Andrej Skerjanec

A thesis submitted to the Faculty of Graduate Studies and Research in partial fulfillment of the requirements for the degree of Doctor of Philosophy.

in

Pharmaceutical Sciences (Pharmacokinetics)

Faculty of Pharmacy and Pharmaceutical Sciences

Edmonton, Alberta

Fall 1995

National Library
of Canada

Acquisitions and
Bibliographic Services Branch

395 Wellington Street
Ottawa, Ontario
K1A 0N4

Bibliothèque nationale
du Canada

Direction des acquisitions et
des services bibliographiques

395, rue Wellington
Ottawa (Ontario)
K1A 0N4

Your file Votre référence

Our file Notre référence

THE AUTHOR HAS GRANTED AN IRREVOCABLE NON-EXCLUSIVE LICENCE ALLOWING THE NATIONAL LIBRARY OF CANADA TO REPRODUCE, LOAN, DISTRIBUTE OR SELL COPIES OF HIS/HER THESIS BY ANY MEANS AND IN ANY FORM OR FORMAT, MAKING THIS THESIS AVAILABLE TO INTERESTED PERSONS.

L'AUTEUR A ACCORDE UNE LICENCE IRREVOCABLE ET NON EXCLUSIVE PERMETTANT A LA BIBLIOTHEQUE NATIONALE DU CANADA DE REPRODUIRE, PRETER, DISTRIBUER OU VENDRE DES COPIES DE SA THESE DE QUELQUE MANIERE ET SOUS QUELQUE FORME QUE CE SOIT POUR METTRE DES EXEMPLAIRES DE CETTE THESE A LA DISPOSITION DES PERSONNE INTERESSEES.

THE AUTHOR RETAINS OWNERSHIP OF THE COPYRIGHT IN HIS/HER THESIS. NEITHER THE THESIS NOR SUBSTANTIAL EXTRACTS FROM IT MAY BE PRINTED OR OTHERWISE REPRODUCED WITHOUT HIS/HER PERMISSION.

L'AUTEUR CONSERVE LA PROPRIETE DU DROIT D'AUTEUR QUI PROTEGE SA THESE. NI LA THESE NI DES EXTRAITS SUBSTANTIELS DE CELLE-CI NE DOIVENT ETRE IMPRIMES OU AUTREMENT REPRODUITS SANS SON AUTORISATION.

ISBN 0-612-06291-0

Canada

University of Alberta

Library Release Form

Name of Author: Andrej Skerjanec

Title of Thesis: Mechanisms of Nonlinear Pharmacokinetics of Mibefradil

Degree: Doctor of Philosophy

Year this Degree Granted: 1995

Permission is hereby granted to the University of Alberta Library to reproduce single copies of this thesis and to lend or sell such copies for private, scholarly, or scientific research purposes only.

The author reserves all other publication and other rights in association with the copyright in the thesis, and except as hereinbefore provided, neither the thesis nor any substantial portion thereof may be printed or otherwise reproduced in any material form whatever without the author's prior written permission.

8819-92ST
Edmonton, Alberta
CANADA
T6C 3P9

Date: 07/07/95

University of Alberta

Faculty of Graduate Studies and Research

The undersigned certify that they have read, and recommend to the Faculty of Graduate Studies and Research for acceptance, a thesis entitled "Mechanisms of Nonlinear Pharmacokinetics of Mibefradil" submitted by Andrej Skerjanec in partial fulfillment of the requirements for the degree of Doctor of Philosophy in Pharmaceutical Sciences (Pharmacokinetics).

Dr. Y.K. Tam, Supervisor

Dr. R.T. Coutts

Dr. F. Jamali

Dr. F. Pasutto

Dr. M. R. Gray

Dr. P. J. McNamara (External Examiner)

Date: JULY 6/1995

DEDICATION

For Simona and our Parents.

ABSTRACT

Mibefradil is a new calcium antagonist under clinical development. A favorable pharmacological profile, demonstrated by high selectivity for coronary arteries and weak negative inotropic effect, brought mibefradil into clinical trials as an antihypertensive and antianginal drug.

Early human pharmacokinetic studies revealed the nonlinear behaviour of mibefradil, characterized by a decrease in oral clearance and an increase in bioavailability with doses increasing from 10 to 320mg, whereas kinetics after 2.5 to 40mg intravenously administered doses were linear. We performed a series of experiments using the dog as an animal model to study the properties and mechanism(s) of nonlinear pharmacokinetics of mibefradil.

To quantify mibefradil in dog plasma and urine samples, we developed an HPLC assay, which proved to be convenient and suitable for use in our studies.

The main trust of our experimentation was to use a chronically instrumented, conscious dog model which allows us to simultaneously monitor the time course of the drug in carotid artery, jugular, portal and hepatic veins with continuous measurement of hepatic blood flow. We showed that complex surgical instrumentation did not compromise liver or any other physiological function in our experimental dogs. Continuous electronic measurements of hepatic blood flow proved to be superior to the noninvasive indocyanine green method.

Preliminary pharmacokinetic studies in intact animals showed that the kinetics of mibefradil after oral administration are nonlinear. This phenomenon is consistent with that observed in humans. We postulated that a reduction in liver first-pass metabolism, an

increase in drug absorption and/or a decrease in presystemic intestinal metabolism may be responsible.

By using the chronically instrumented conscious dog model, the involvement of organs such as the gut and the liver in nonlinear first-pass effect was evaluated and quantified. First, we found that liver is the major organ for eliminating mibefradil and second, the dose dependent increase in bioavailability is due to a reduction in hepatic extraction but not due to a dose-dependent increase in gut absorption. Reduction in liver clearance and volume of distribution was observed with increasing oral doses and these changes were related to the dose and duration of the treatment. An important finding was that even when equal intravenous and oral doses were used, the conventional area ratio approach produced inaccurate absolute bioavailability values, because systemic clearance is dependent upon the cumulative exposure of the liver to the drug, which is higher after oral administration. Our data suggest that dose and time-dependent changes of mibefradil kinetics in dogs are consistent with saturation of tight binding to hepatic tissue, metabolic alteration such as inactivation of hepatic CYP enzyme(s) and/or metabolic product inhibition.

ACKNOWLEDGEMENTS

The author thanks Dr. Yun K. Tam for his exceptional and patient guidance throughout my graduate studies at the University of Alberta.

Sincere thanks are due to Dr. Soheir Tawfik for her surgical expertise and technical assistance with my mibefradil experiments. Stella Ngo assisted Soheir with surgical procedures and her help is greatly acknowledged. Dr. Darryl O'Brien was involved with the surgical and experimental portion of the indocyanine green studies. Working with him was a pleasant experience.

This work was supported in part by the Medical Research Council of Canada and Hoffmann La Roche, Basel, Switzerland.

TABLE OF CONTENTS

1. INTRODUCTION 1

1.1 Calcium and Calcium Channels 2

1.2 Calcium Channel Antagonists 6

1.3 Pharmacology of Mibefradil 7

1.4 Pharmacokinetics of Mibefradil 11

1.4.1 Studies in Healthy Human Volunteers 11

1.4.2 Protein Binding in Human and Dog Plasma 12

1.4.3 Qualitative Metabolic Studies in Rats 12

1.5 Determination of Mibefradil in the Biological Fluids 12

1.6 Nonlinear Pharmacokinetics 13

1.6.1 Linear and Nonlinear Systems 13

1.6.2 Relationship between AUC and the Dose 13

1.6.3 Less than Proportional Increase in AUC 15

1.6.4 Greater than Proportional Increase in AUC 15

1.6.4.1 Michaelis-Menten Kinetics 16

1.6.4.2 Dose and Time-Dependent Kinetics 17

1.6.5 Nonlinear Kinetics and Absolute Bioavailability 18

1.6.6 Nonlinear Kinetics and Mibefradil 19

1.7 Chronically Instrumented Conscious Dog Model 19

1.7.1 Hepatic Blood flow Measurements in a Conscious Dog Model 20

1.7 Hypotheses 21

1.8 Objectives 22

2. EXPERIMENTAL SECTION 28

2.1 Chemicals and Assay Procedures 28

2.1.1 HPLC Assay of Mibefradil in Dog Plasma and Urine 28

2.1.1.1 Standard solutions 28
2.1.1.2 Sample preparation 29
2.1.1.3 Instrumentation and chromatographic conditions 30
2.1.1.4 Calibration curves and assay validation 30
2.1.2 Indocyanine Green Studies 31
2.2 Instrumentation 32
2.2.1 Blood Flow Measurements 32
2.3 Surgery, Postoperative Care and Catheter Maintenance 32
2.3 Design of Animal Experiments 33
2.3.1 Blood Flow Measurements and Indocyanine Green Kinetics 34
2.3.2 Mibefradil Pharmacokinetic Studies 35
2.3.2.1 Experimental protocol 35
2.3.2.2 Intravenous Dosing - Noninstrumented Dogs 36
2.3.2.3 Intravenous Dosing - Instrumented Dogs 36
2.3.2.4 Oral Dosing - Noninstrumented Dogs 37
2.3.2.5 Oral Dosing - Instrumented Dogs 38
2.3.2.6 Plasma Protein Binding Studies in Dogs 38
2.4 Data Analysis 39
2.4.1 Pharmacokinetic Analysis 39
2.4.1.1 Blood Flow Measurements and Indocyanine Green Kinetics 39
2.4.1.2 Mibefradil - Noninstrumented Dogs 41
2.4.1.4 Mibefradil - Instrumented Dogs: Measurement of Physiological Kinetic Parameters 42
2.4.2 Statistical Analysis 45
2.4.2.1 Blood Flow Measurements and Indocyanine Green Kinetics 45
2.4.2.2 Mibefradil Pharmacokinetics in Noninstrumented and Instrumented Dogs 45

3. RESULTS 46

3.1 HPLC Assay of Mibefradil in Dog Plasma and Urine 46

3.2 Blood Flow Measurements and Indocyanine Green Kinetics 47
3.3 Mibefradil Pharmacokinetics in Noninstrumented Dogs 48
3.3.1 Intravenous Study 48
3.3.2 Oral Study 48
3.4 Mibefradil Pharmacokinetics in Instrumented Dogs 49
3.4.1 Jugular vein intravenous and oral data 49
3.4.2 Pharmacokinetic analysis based on measurement of physiological kinetic parameters 50
3.5 Plasma Protein Binding Studies in Dogs 53

4. DISCUSSION 75
4.1 HPLC Assay of Mibefradil in Dog Plasma and Urine 75
4.2 Blood Flow Measurements and Indocyanine Green Kinetics 75
4.3 Mibefradil Pharmacokinetics in Noninstrumented Dogs 79
4.4 Mibefradil Pharmacokinetics in Instrumented Dogs 83

5. SUMMARY AND CONCLUSIONS 90

6. REFERENCES 93

LIST OF TABLES

Table 1.1 Summary of pharmacokinetic parameters of mibefradil after intravenous and oral administration of single doses to healthy human volunteers (n=48, BW=74.4±7kg, age=25±2yrs). Data extracted from *Welker et al., 1989*. 23

Table 3.1 Accuracy and precision of the assay for mibefradil in plasma (PL) and urine (UR). 54

Table 3.2 Comparison of indocyanine green pharmacokinetic parameters before and after the instrumentation. 55

Table 3.3 Pharmacokinetic parameters for chronically instrumented dogs that underwent the ICG treatment. Electronically measured blood flows in hepatic artery (Q_{HA}), portal vein (Q_{PV}), sum of arterial and portal blood flow (Q), ICG based hepatic blood flow (Q_{ICG}) and ratio between ICG estimated and electronically measured hepatic blood flows. 56

Table 3.4 Food effect on electronically and ICG measured hepatic blood flow (Q and Q_{ICG}) and ICG disposition characteristics. 57

Table 3.5 Mibefradil pharmacokinetic parameters in four dogs after single intravenous doses of 1 mg/kg and three oral doses of 1, 3 and 6 mg/kg. 58

Table 3.6 Mibefradil jugular vein based pharmacokinetic parameters in four instrumented dogs after single intravenous doses of 1 mg/kg, three single oral doses of 1, 3 and 6 mg/kg and multiple doses of 3 mg/kg, q12h for 8 days. . 59

Table 3.7 Mibefradil pharmacokinetic parameters in four instrumented dogs after single intravenous doses of 1 mg/kg, three single oral doses of 1, 3 and 6 mg/kg and multiple doses of 3 mg/kg twice a day for 8 days. Fraction of the dose absorbed through the gut (F_a), absorption rate constant (K_a) and % total amount absorbed at a rate constant corresponding to K_a. Time at which a maximum concentration occurs (T_{max}) is reported for hepatic (HV), portal (PV) and jugular vein (JV) catheters. 60

Table 3.8 Mibefradil pharmacokinetic parameters in four instrumented dogs after single intravenous doses of 1 mg/kg, three single oral doses of 1, 3 and 6 mg/kg and multiple doses of 3 mg/kg. Calculations are based on electronically measured hepatic blood flows and plasma profiles in carotid artery, portal and hepatic vein (see section *2.4.1.4* for detailed description). 61

LIST OF FIGURES

Figure 1.1 Structure of mibefradil (* denotes the chiral center), (1S,2S)-2-[2-[[3-(2-benzimidazolyl)propyl]methylamino]ethyl]-6-fluoro-1,2,3,4-tetrahydro-1-isopropyl-2-naphthyl methoxyacetate..... 24

Figure 1.2 Structure of internal standard (* denotes the chiral center). Internal standard is the S,S-isomer..... 24

Figure 1.2 The regulation of Ca^{2+} in myocardium. TT denotes transverse tubule, SR sarcoplasmic reticulum and Mit. mitochondrion. Numbers in circles denote the mechanisms affecting intracellular Ca^{2+} (*Braunwald, 1982*)..... 25

Figure 1.4 Relationship between the AUC (left panel), C_{max} (right panel) and the dose after single oral doses to humans (for clarity. doses were normalized for body weight). Adapted from Welker et al. 1989. 27

Figure 3.1 Representative chromatograms of blank dog plasma (upper panel) and dog plasma sample taken at 36h after 3 mg/kg single oral dose of mibefradil (I) (lower panel). The concentration of mibefradil corresponds to 12 ng/ml. II denotes internal standard. 62

Figure 3.2 Representative chromatograms of blank dog urine (upper panel) and dog urine sample collected between 12-24 hours after a single oral dose of 6 mg/kg of mibefradil (I) (lower panel). The concentration of mibefradil corresponds to 64 ng/ml. II denotes internal standard..... 63

Figure 3.3 (A) ICG plasma vs. time profile in a representative dog; jugular vein (●), carotid artery (o), portal vein (▲), hepatic vein (□). (B) Electronically measured blood flow rates during the ICG experiments in dogs; total liver flow (●), portal vein flow (o), hepatic artery flow (▼). Each data point represents the mean (±SEM) of seven dogs..... 64

Figure 3.4 Plasma concentration vs. time profile of mibefradil in 3 dogs after (**A**) intravenous (•) and (**B**) oral administration..... 65

Figure 3.5 Relationship between the (**A**) AUC, (**B**) C_{max}, and the dose after single oral doses to 3 dogs..... 66

Figure 3.6 Plasma concentration vs. time profile of mibefradil in four dogs after (**A**) intravenous administration of 1 mg/kg dose and (**B**) oral administration of 1, 3, 6 mg/kg single and 3 mg/kg multiple doses to 4 dogs..... 67

Figure 3.7 Plasma concentration vs. time profile of mibefradil in four catheters after 3 mg/kg single oral dose in a representative dog. (JV) Jugular vein, (CA) Carotid artery, (PV) Portal vein, (HV) Hepatic vein..... 68

Figure 3.8 Plot of % amount of mibefradil to be absorbed vs. time after oral administration of single 1, 3 and 6 mg/kg doses and multiple 3 mg/kg doses.69

Figure 3.9 Time course of the mean hepatic extraction ratio after 1 mg/kg intravenous and oral administration of 1, 3 and 6 mg/kg single and 3 mg/kg multiple oral doses in four dogs. Upper panel comprises the entire time course of the drug in the body, lower panel represents the first 360 min time profile. (For clarity, only mean values are depicted.)..... 70

Figure 3.10 Time course of the average increase (%) in hepatic arterial blood flow (upper panel) and average increase (%) in hepatic blood flow (lower panel) during the first 360 min after 1 mg/kg intravenous and oral administration of 1, 3 and 6 mg/kg single and 3 mg/kg multiple oral doses in four dogs. (For clarity, only mean values are depicted.)..... 71

Figure 3.11 Time course of the mean hepatic clearance after 1 mg/kg intravenous and oral administration of 1, 3 and 6 mg/kg single and 3 mg/kg multiple oral doses in four dogs. Upper panel comprises the entire time course of the drug in the body, lower panel represents the first 360 min time profile. (For clarity, only mean values are depicted.)..... 72

Figure 3.12 Plot of mean hepatic clearance vs. mibefradil plasma concentration in post-absorption, post-distribution phase. Hepatic clearance values were obtained at 15ng/ml mibefradil plasma concentration, after 1mg/kg intravenous and 1, 3 and 6mg/kg single oral doses. Hepatic clearance value at 80ng/ml is shown for 6mg/kg oral dose and for multiple doses at 370ng/ml. Each data point represents an average value from four dogs. Hepatic clearance after 3 and 6mg/kg single and 3mg/kg multiple oral doses was significantly different from the intravenous treatment ($P<0.05$). Single 1mg/kg dose was different from 6mg/kg oral dose at 15ng/ml ($P<0.05$). Hepatic clearance after multiple doses was different from all but 6mg/kg oral dose ($P<0.05$). 73

Figure 3.13 Cumulative exposure of the liver to mibefradil after 1 mg/kg intravenous and oral dose to four dogs. 74

GLOSSARY OF ABBREVIATIONS AND SYMBOLS

α	probability of making a type I error
ANOVA	analysis of variance
AUC	area under the plasma concentration-time curve from 0 to ∞
AUC_{po}	area under the plasma concentration-time curve after oral dose
AUC_{iv}	area under the plasma concentration-time curve after intravenous dose
AUMC	area under the first moment curve
β	terminal elimination rate constant
BW	body weight
C	plasma drug concentration
C_0	plasma drug concentration at t=0 after i.v. dose, 1 comp. model
C_{JV}	plasma drug concentration in jugular vein
C_{CA}	plasma drug concentration in carotid artery
C_{HV}	plasma drug concentration in hepatic vein
C_{PV}	plasma drug concentration in portal vein
Cl/F	oral clearance
Cl_B	blood systemic clearance
Cl_i	intrinsic clearance
Cl_H	hepatic clearance
Cl_S	systemic clearance
cm	centimeter(s)
C_{max}	maximum (peak) concentration
CV	coefficient of variation
°C	degrees Celsius
D_{iv}	intravenous dose
D_{po}	oral dose
E_H	hepatic extraction ratio
E_L	lung extraction ratio
EDTA	disodium ethylenediaminetetraacetate

eq.	equation
F	absolute bioavailability
F_a	fraction of the dose absorbed into the portal circulation
F_H	hepatic availability
F_L	lung availability
f_u	fraction of unbound drug in plasma
f	female
g	gram(s)
g	gravity
HA	hepatic artery
Hct	haematocrit
HV	hepatic vein
h	hour(s)
HPLC	high-performance liquid chromatography
ICG	indocyanine green
id	inside diameter
inf	infinity
iv	intravenous
JV	jugular vein
K_a	first-order absorption rate constant
K_e	first-order elimination rate constant
k	first-order metabolic rate constant
kg	kilogram(s)
K_m	Michaelis constant
l	liter(s)
M	molar
µg	microgram(s)
µl	microliter(s)
m	male
mg	milligram(s)

min	minute(s)
ml	milliliter(s)
MRT	mean residence time
n	number of observations
ng	nanogram(s)
nm	nanometer
P	probability of rejecting the null hypothesis when it is true
pK_a	negative logarithm of equilibrium constant of acid
pH	negative logarithm of concentration of H^+ ions
po	oral
PV	portal vein
Q_H	hepatic blood flow
Q_{HA}	hepatic artery blood flow
Q_{PV}	portal vein blood flow
QC	quality control
r^2	coefficient of determination
SD	standard deviation
SEM	standard error of the mean
$\int$	integral
%	percent
$t_{1/2}$	half-life
T_{max}	time to maximum (peak) concentration
U	unit(s)
V_β	volume of distribution based on AUC method
V_d	volume of distribution based on 1 compartment open model
V_m	maximum velocity of metabolism
V_{ss}	volume of distribution at steady-state

1. INTRODUCTION

Calcium channel antagonists are widely used therapeutic agents for the treatment of various cardiovascular ailments. They are one of the standard first-line treatments for essential hypertension. In combination with β-blockers and nitrates, they have become established therapy for angina pectoris (*Opie, 1991*). Verapamil, diltiazem and nifedipine are the most known prototypes of the first-generation calcium channel antagonists. Their main pharmacokinetic and pharmacodynamic characteristics are low bioavailability and relatively short duration of action (*Echizen & Eichelbaum, 1986*; *Hermann & Morselli, 1985*). In recent years much effort was oriented towards developing new agents with improved kinetic and dynamic profiles. Mibefradil (code Ro 40-5967; Hoffmann La Roche, Basel, Switzerland), a benzimidazolyl-substituted tetraline derivative, is a new calcium antagonist under development. The structure of this drug is shown in Figure 1.1. Mibefradil is a base with a pK_a value of 4.8 for the benzimidazolyl group and 5.5 for the tertiary amine, and with a high partition coefficient (octanol-buffer, pH=7.3 at 22° C: >1000) (*Osterrieder & Holck, 1989*; *Clozel & Kleinbloesem, 1989*). The molecule has two asymmetric carbon atoms and among the four stereoisomers, 1S,2S has undergone clinical development (*Clozel et al. 1989*). Preclinical experiments have shown that mibefradil has antiischemic and antihypertensive properties (*Clozel et al. 1989*; *Hefti et al. 1990*). Moreover, mibefradil, with only weak negative inotropic effects on the myocardium (*Osterrieder & Holck, 1989*) differs from other calcium antagonists by a marked selectivity of its action on coronary arteries versus peripheral arteries. Due to this

pharmacological profile, mibefradil was proposed for clinical trials as an antihypertensive and antianginal drug (*Hefti et al. 1990*).

1.1 Calcium and Calcium Channels

Calcium ions (Ca^{2+}) are vital in many biologic processes, including a variety of enzymatic reactions, activation of excitable cells, coupling of electrical activation to cellular secretion, homeostasis and the metabolism of bone (*Braunwald, 1982*). At the cellular level, Ca^{2+} is regulated at both plasmalemmal and intracellular loci (*Triggle, 1990*). Intracellular free Ca^{2+} concentration plays an important role as a messenger for cellular functions under both normal and pathological conditions. In resting myocardial and smooth muscle cells, the intracellular concentration of free Ca^{2+} is ~ 5×10^{-8} M or less and rises to ~ 5×10^{-7} M during cell excitation. At this higher free concentration, Ca^{2+} binds to proteins troponin and calmodulin (*Braunwald, 1982*). This binding allows interaction between myosin and actin in the presence of ATP and results in muscular contraction. When intracellular free Ca^{2+} concentration is reduced, Ca^{2+} is dissociated from the binding proteins. This causes the actin-myosin cross-link to break and subsequent muscular relaxation. Thus the isometric myocardial systolic and diastolic tensions are directly related to the myoplasmic free Ca^{2+} concentration. To control the level of intracellular free Ca^{2+}, a set of processes is coordinated by the cell. These processes in myocardium are represented schematically in Figure 1.2 (*Braunwald, 1982*). The main sources and storehouses for intracellular Ca^{2+} mobilization and sequestration are located at the infoldings of the surface membrane (the transverse tubular system), the mitochondria and

particularly the sarcoplasmic reticulum. The initial influx of Ca^{2+} across the transverse tubular membrane through channels (mechanism 1A and 1B) triggers the secondary and much larger release of Ca^{2+} from the sarcoplasmic reticulum, followed by activation of the contractile system. It was proposed that a "voltage sensor" is located in the transverse tubular membrane and controls the release of calcium from the sarcoplasmic reticulum (*Schneider & Chandler, 1973*). In response to changes of transverse-tubular potential, the voltage sensor undergoes molecular rearrangement and controls calcium flow from the sarcoplasmic reticulum. Other pathways of movement of Ca^{2+} across sarcolemma includes bi-directional Na^{+}-Ca^{2+} exchange (mechanism 2), Ca^{2+} leak pathways (mechanism 6) and extrusion of Ca^{2+} (mechanism 3). Intracellular Ca^{2+} can be taken up into the lumen of sarcoplasmic reticulum (mechanism 4) and other intracellular structures such as mitochondria (mechanism 5).

The sarcolemmal channels represent a very selective and important pathway of Ca^{2+} influx into excitable cells (*Triggle, 1990; Bean, 1989*) and are termed "calcium channels". Voltage-dependent calcium channels mediate the influx of Ca^{2+} in response to membrane depolarization and play a vital role in excitation-contraction coupling of cardiac and smooth muscle (*Hagiwara & Byerly, 1981*). In the receptor-operated calcium channels, the receptor and the channel may belong to the same protein(s) or the receptor and the channel may be physically separate and connected through cytosolic or membrane messengers (*Triggle, 1990*). The indication of a receptor-operated voltage-independent channel in the vascular smooth muscle is weak (*Benham & Tsien, 1988*). The beta-adrenergic agonist-induced stimulation of the myocardium still needs voltage stimulation

to open the channel (*Schneider & Sperelakis, 1975*). Thus the voltage-dependent channels may be considered the only type of calcium channels in the myocardium.

The influx of positively charged calcium ions is associated with an electric current, called the calcium current. The rates of activation and inactivation of this inward calcium current are slower than those of the fast inward current produced by influx of Na^+ (*Carmeliet, 1980*) and thus the calcium current is also known as "slow inward current". The calcium current plays a critical role in the generation and maintenance of the plateau of the cardiac action potential, allowing more cytosolic free Ca^{2+} to trigger contraction (*Fozzard, 1983*).

Sinoatrial (SA) pacemaker cells and atrioventricular (AV) automatic cells have slowly rising action potentials and a reduced rate of conduction (*Braunwald, 1982*). Both automaticity and conduction in SA and AV node are largely mediated by transmembrane influx of Ca^{2+} through calcium channels (*Wit & Cranefield, 1974*; *Zipes & Fischer, 1974*). Thus the calcium channel is not only involved in vascular and cardiac muscle contraction but is also involved in conduction of impulses and in pacemaker activity of the nodal tissue. Process that modify calcium current will have important effects on SA and AV nodes.

The calcium channels are divided into three subtypes, termed L, T, and N channels based on their voltage threshold for activation, conductances and inactivation characteristics (*Fox et al. 1987*; *Triggle, 1994*). The L-type channels, characterized by high threshold, large conductance and slow inactivation (long-lasting, or L-type), are involved in maintenance of the action potential plateau. The T channels have low

threshold and low conductance. They are rapidly inactivated (transient, or T-type) and are involved in pacemaking and trigger functions. The N (nervous) channels are found in neurons, have properties in between those of the L and T channels, and are involved in release of neurotransmitters from nerve terminals (*Miller, 1987*; *Wagner et al. 1988*; *Carmeliet, 1988*).

The predominant type of voltage-dependent calcium channel in cardiac muscle cells is the L type channel (*Catterall et al. 1989*; *Hosey et al. 1989*). These channels appear to be also present in high density in skeletal muscle transverse tubule membranes. The kinetics of opening and closing of L channels in cardiac cells are quite different from those in skeletal muscle. The subtypes of L channels are possible and structural differences may be responsible for the observed differences in properties.

In contrast to L-type Ca^{2+} channel, T-type channel is only superficially understood and is found in relatively high density in spontaneously active vascular muscle (*Bean, 1989*; *Hermsmeyer, 1991*). A comparison of T-type Ca^{2+} channels with L and N types shows that the sensitivity to a specific blocker is missing, and only inorganic ions (Ni^{2+}) or drugs with other primary mechanisms of action (amiloride, alcohols) can only partially block T-type channels (*Tsien et al. 1988*; *Triggle, 1994*).

1.2 Calcium Channel Antagonists

Although specific drugs may interact with each of the calcium control processes shown in Figure 1.2 , in practice, only one class of drugs interacting at the plasmalemmal voltage-dependent calcium channels is therapeutically useful. Fleckenstein (*Fleckenstein, 1977*) found that some compounds can selectively block the excitation-contraction coupling in heart muscle. This blocking effect can be overcome by agents that increase the supply of Ca^{2+}, and by Ca^{2+} itself. Because of their specific antagonism to the movement of extracellular Ca^{2+}, they were called calcium channel entry blockers or calcium antagonists. Calcium channel entry blockers are chemically heterogeneous and include benzothiazepine, phenylalkylamine and dihydropyridine derivatives.

The L type calcium channel which is responsible for calcium entry during the plateau of the action potential is sensitive to diltiazem, nifedipine and verapamil, the three prototypes of calcium channel antagonists. These three agents, with different molecular structures, bind at an allosterically linked set of sites on a major protein of the L class of vascular and myocardial calcium channels. These sites represent the active part of the calcium channel and interaction at these sites blocks channel function. Mibefradil, which is chemically different from other calcium channel antagonists, binds to the [^{3}H]desmethoxyverapamil receptor at (or near) the Ca^{2+} channel (*Osterrieder & Holck, 1989*). However, it has been shown (*Mishra & Hermsmeyer, 1994*) that mibefradil also acts upon T-type Ca^{2+} channels and proved to be the first Ca^{2+} channel blocker to eliminate dihydropyridine-insensitive voltage-dependent Ca^{2+} current at concentrations which elicited only 25% to 70% block of L-type Ca^{2+} currents.

1.3 Pharmacology of Mibefradil

Mibefradil binds to the [^{3}H]desmethoxyverapamil receptor at (or near) the Ca^{2+} channel in cardiac cell membranes of guinea pig (*Osterrieder & Holck, 1989*). However, the striking pharmacological difference between mibefradil and verapamil is their effect on cardiac contractility. Mibefradil is 30 times less potent as a negative inotropic agent in isolated, electrically stimulated left atria of guinea pig than verapamil (*Osterrieder & Holck, 1989*). The weak inotropic effect of mibefradil as compared to that of verapamil has also been observed in the rat *in vitro* and *in vivo* (*Clozel et al. 1990*). Because of its very low negative inotropism and its lack of reflex tachycardia (characteristic of dyhidropyridines), mibefradil seems to have a unique hemodynamic profile among calcium antagonists (*Osterrieder & Holck, 1989*). There appears to be a preference of mibefradil for the coronary vasculature, suggesting greater affinity for Ca^{2+} channels of the coronary blood vessels than for those of peripheral blood vessels (*Osterrieder & Holck, 1989*). Moreover, the membrane effects of mibefradil on dog coronary and saphenous arterial vascular muscle cells showed that mibefradil acts with selectivity for coronary over saphenous arteries (*Bian & Hermsmeyer, 1993*). Mibefradil had only a minor effect on contraction frequency of rat myocardial cells while significantly inhibiting spontaneous contractions of rat spontaneously active coronary muscle cells (*Mishra & Hermsmeyer, 1994*). This is very interesting, because tissue selectivity (vascular smooth muscle vs. myocardium) is well known for the dihydropyridine-type Ca^{2+} channel blockers such as nifedipine (*Godfraind et al. 1988*). Mibefradil appears to be the first calcium antagonist acting through the verapamil binding site, which exhibits a degree of vascular selectivity

similar to that of dihydropyridines. A calcium channel blocker with high selectivity for coronary vascular tissue and devoid of negative inotropic effect would represent a very promising agent for the treatment of arterial hypertension, cardiac arrhythmias and conditions related to myocardial infarction.

Arterial hypertension is associated with an intimal dysfunction characterized by endothelium-dependent constriction to serotonin, decreased endothelium-dependent relaxation to acetylcholine, and a subendothelial infiltration of monocyte-macrophages (*Gray et al. 1993*). Animal studies showed that long-term treatment (4 weeks) with mibefradil reverses both the functional and morphological changes of the aortic intima in spontaneously hypertensive rats (*Gray et al. 1993*) by evoking endothelium-dependent relaxations and inhibiting endothelium-dependent contractions (*Boulanger et al. 1994*). In hypersensitive blood vessels, the former are attenuated and the latter are augmented (*Lüscher & Vanhoutte, 1990*). Although it is difficult to extrapolate from the present *in vitro* observations to the intact organism, the combined action of mibefradil on both aspects of endothelium-dependent responses may help explain its antihypertensive properties *in vivo* (*Clozel et al. 1990*; *Hefti et al. 1990*).

Recent studies have shown that a calcium-dependent inward current is required for the initiation of ventricular fibrillation (*Kihara & Morgan, 1991*; *Merillat et al. 1990*), and that Ca^{2+} channel antagonists can prevent malignant arrhythmias in animals (*Billman, 1989*) and reduce mortality in cardiac patients (*Anonymous, 1990*; *Boden et al. 1991*). For example, diltiazem was found to decrease cardiac mortality in myocardial infarction patients with well preserved cardiac function. However, diltiazem increased mortality in

patients with radiographic evidence of pulmonary congestion (*Boden et al. 1991*). Calcium channel antagonists, therefore, may have untoward effects in patients with compromised cardiac function. In contrast to verapamil and diltiazem, mibefradil does not adversely affect myocardial force during heart failure in models of myocardial ischemia in dogs (*Clozel et al. 1989*), hypertrophied and failing rabbit heart (*Ezzaher et al. 1991*) and in rats with chronic myocardial infarction (*Veniant et al. 1991*), suggesting that it may also represent a safer alternative for arrhythmia management in these high risk patients. This aspect was adressed in a study where the effects of mibefradil on the susceptibility to ventricular fibrillation in dogs were investigated (*Billman, 1992*). Results showed that mibefradil can protect against ventricular fibrillation without significant negative inotropic or dromotropic effects. The mechanism is yet to be fully understood, however it has been demonstrated (*Fang & Osterrieder, 1991*) that in depolarized cells, mibefradil demonstrated high potency in the inhibition of calcium entry. It is well established that cardiac cells depolarize during myocardial ischemia (*Levy, 1989*). Therefore, mibefradil may be particularly selective for ischemic tissue, the tissue most vulnerable to calcium overload and arrhythmia formation. Study on the effects of mibefradil in a canine model of chronic coronary artery stenosis indicate that mibefradil has an antiischemic effect in the clinically relevant setting of exercise-induced regional myocardial ischemia (*Guth, 1992*) and was as effective as verapamil in limiting infarct size during the period of regional ischemia (*Vander Heide et al. 1994*). These observations coupled with less negative inotropy suggest that mibefradil may have greater therapeutic potential for use in patients with acute myocardial infarction than the classical antagonists.

Little information has been published so far on the *in vivo* quantification of the antihypertensive effect in relation to the dose and duration of treatment. Antihypertensive effect of mibefradil on systolic arterial blood pressure and heart rate was investigated in conscious spontaneously hypertensive rats, renal hypertensive rats, deoxycorticosterone acetate (DOCA)-NaCl hypertensive rats and normotensive Wistar rats. After single oral doses (10-30 mg/kg), mibefradil produced a dose-related decrease in blood pressure in all three types of hypertensive rats. The antihypertensive effects of mibefradil occurred within 1 h and reached maximal values 3 h postdose. Significant antihypertensive effect of mibefradil (30 mg/kg) persisted for 24 h, suggesting that mibefradil might be suitable for clinical use as a once-a-day antihypertensive agent (*Hefti et al. 1990*). Tolerability, hemodynamic and humoral effects related to a once a day use was tested in patients with hypertension (*Schmitt et al. 1992*). Ascending oral doses of 50, 100, 150, or 200 mg were administered once daily for 8 days in a solution. Mibefradil was well tolerated up to 150 mg and blood pressure was dose-dependently reduced over the full 24-hour dosing period with more pronounced effects on day 8 than on day 1 and the maximum blood pressure reduction was obtained after 150 mg dose. Concentration-effect analysis showed that relevant atrioventricular conduction disturbances occur only at concentrations much higher than those required to reduce blood pressure. Data suggest that optimal blood pressure control can be achieved with doses of 50 to 100 mg during long-term treatment (*Schmitt et al. 1992*).

1.4 Pharmacokinetics of Mibefradil

1.4.1 Studies in Healthy Human Volunteers

Early human studies (*Welker et al. 1989*) after 2.5 mg intravenous dose showed that mibefradil is slowly eliminated from the body, mainly due to extensive distribution of the drug in the body, V_{ss}=278 (104-418) l, and low systemic clearance, Cl_s=288 (209-436) ml/min, resulting in a half-life of 14.9 (8.4-24.6) h. Urinary excretion of intact drug is negligible. A portion of the data from the study is summarized in Table 1.1. The study showed that single dose kinetics of mibefradil are linear after intravenous administration of 2.5 to 40 mg doses; whereas nonlinear disposition pattern was observed after single oral doses, ranging from 10 to 320 mg. Pharmacokinetic data after single 10 mg oral dose showed that bioavailability is low, F=0.37 (0.15-0.90). This is unexpected in the view of a low systemic clearance of mibefradil. A 0.37 bioavailability at 10 mg dose would therefore suggest an incomplete absorption and/or gut metabolism. Nonlinear behaviour was characterized by a decrease in oral clearance and an increase in bioavailability (dose normalized AUC_o/AUC_{iv} ratio) with increasing dose (Figure 1.3). As a result of nonlinear oral clearance, greater than proportional increase in area under the plasma mibefradil concentration vs. time, AUC_o, and maximum peak concentration, C_{max}, was observed with increasing oral doses (Figure 1.4).

1.4.2 Protein Binding in Human and Dog Plasma

Mibefradil is highly bound to the plasma proteins in man and dog (*Brand & Meyer, 1988*). Using the *in vitro* ultrafiltration method, studies showed that the free fraction in human plasma was 0.32% and the binding remained constant up to the 2000 ng/ml range. The free fraction of mibefradil in dog plasma was three times higher and the linear range was up to 4000 ng/ml.

1.4.3 Qualitative Metabolic Studies in Rats

Metabolism in rats has been intensively investigated (*Wiltshire et al. 1992*) and appears to be complex, giving rise to a multitude of products. Major metabolic pathways include *N*-demethylation, hydrolysis of the ester side chain, hydroxylation, aromatization of the tetrahydronaphthyl system, loss of benzimidazole and glucuronidation of hydroxyl groups. The resultant metabolites are predominantly excreted into the bile. However, the relative contribution of individual metabolic pathways was not quantified.

1.5 Determination of Mibefradil in the Biological Fluids

A published assay, describing the measurement of mibefradil in biological fluids was not available at the time when the project begun. Therefore, a suitable analytical method for the quantification of mibefradil in plasma and urine was sought.

1.6 Nonlinear Pharmacokinetics

1.6.1 Linear and Nonlinear Systems

Mathematically, the body can be considered as an operator that transforms the input (dose rate) into output (plasma concentration of drugs). A linear system exists when input-output relationships are fully described by one or more linear equations. The most important feature of a linear system is that it obeys the law of superposition, which states that in a linear system the output produced by several simultaneously applied inputs is equal to the sum of the outputs of separately applied inputs (*Levy & Gibaldi, 1975*). In essence, each dose of drug acts independently of every other dose, that the rate and extent of absorption and average systemic clearance are the same for each dosing interval, and that linear pharmacokinetics apply so that a change in dose during the multiple dosing regimen can be accommodated (*Gibaldi & Perrier, 1982*). A system is said to be non-linear when it does not conform to these principles.

1.6.2 Relationship between AUC and the Dose

The proportionality between the dose (input) and AUC (output) of a drug is an important criterion used to determine whether the drug exhibits linear or nonlinear kinetics in the body (*Lin, 1994*). Practically, nonlinear pharmacokinetics are reflected most commonly in a less than or greater than proportional increase in the area under the drug concentration-time curve (AUC) with an increase in dose (*Ludden, 1991*). The AUC following oral administration can be described by the following relationship:

$$AUC = \frac{F_a * F_H * F_L * Dose}{Cl_S} \quad (1.1)$$

where F_a, F_H, F_L and Cl_S depict the fraction of the dose absorbed, fraction of the drug escaping liver metabolism, fraction of the drug escaping lung metabolism and systemic clearance, respectively. Assuming the well-stirred model and liver is the main determinant of systemic clearance, substituting Cl_S with Cl_H , the expression for AUC in eq. 1.1 becomes:

$$AUC = \frac{F_a * F_H * Dose}{Cl_H} \quad (1.2)$$

where $Cl_H = Q_H * E_H$ (1.3)

and $E_H = \frac{Cl_i * f_u}{Q_H + Cl_i * f_u}$ (1.4)

With appropriate substitution of CL_H and E_H values from eq. 1.3 and 1.4 into eq. 1.2, the following relationship is obtained:

$$AUC = \frac{F_a * Dose}{Cl_i * f_u} \quad (1.5)$$

where Cl_H, Q_H and E_H are liver clearance, blood flow-rate and extraction ratio, respectively. Cl_i is a free hepatic intrinsic clearance and f_u is the fraction of unbound drug in plasma. As indicated in eq. 1.5, AUC after an oral dose is affected not only by absorption but also by elimination and protein binding.

1.6.3 Less than Proportional Increase in AUC

Since the concentration of drug in plasma after oral dosing is a function of both absorption and elimination, the AUC is a net result of both processes. Thus a less than proportional increase in AUC may be due to an increase in elimination as well as to a decrease in absorption. We first consider dose-dependent absorption. There are at least three processes that can cause a dose-dependent decrease in absorption: 1) decrease in dissolution rate (*Barrett & Bianchine, 1975*; *Dressman & Fleisher, 1986*; *Dressman et al. 1984*), 2) decrease in transit time of drugs remaining in the regions of the gastrointestinal tract (*Chen et al. 1992*) and 3) the ability or inability of drugs to cross intestinal barriers (*Amidon et al. 1986*; *Chungi et al. 1978*). For low clearance drugs, binding is an important determinant in drug elimination, and total body clearance is directly proportional to the unbound fraction in plasma (*Wilkinson & Shand, 1975*). Saturation of protein binding of a drug may therefore result in enhanced elimination. Increased rate of elimination may occur as a result of autoinduction of metabolism in which the elimination clearance of a drug increases following multiple doses and the increase in clearance is greater after a high dose than after a low dose (*Bertilsson et al. 1980*; *Reilly et al. 1978*; *Levy, 1986*).

1.6.4 Greater than Proportional Increase in AUC

This phenomenon can be attributed to a decrease in elimination and an increase in absorption. Many drugs undergo significant presystemic metabolism or degradation in the

gut lumen (*Skerjanec et al. 1995*), gut mucosa (*George, 1981*) or the liver (*Pond & Tozer, 1984*). If one or more of these processes is altered (reduced) as the dose increases, a greater than proportional increase in AUC with the dose may result (*Wagner, 1985*; *Shand & Rangno, 1972*; *Walle et al. 1978*). Reduction in elimination capacity is often attributed to concentration dependent or Michaelis-Menten type kinetics (*Sheiner & Ludden, 1992*) but others, which are not consistent with the Michaelis-Menten kinetics have been reported. They are termed dose and time-dependent processes (*Klotz & Reimann, 1981*; *Klotz et al. 1976*; *Levy, 1986*; *Hussain et al. 1994*; *Saville et al. 1989*).

1.6.4.1 Michaelis-Menten Kinetics

The rate of an enzymatic process such as biotransformation can usually be described by the Michaelis-Menten equation:

$$Rate\ of\ elimination = \frac{V_{max} * C}{K_m + C} \tag{1.6}$$

where C is the drug concentration in the plasma, V_{max} is the maximum production rate of metabolite, and K_m is the Michaelis constant. The constant V_{max} is a function of the total amount of metabolizing enzyme while K_m reflects the affinity between drug (substrate) and enzyme. If a plasma concentration is much smaller than the K_m value, it follows from eq. 1.6 that:

$$Rate\ of\ elimination = \frac{V_{max}}{K_m} * C = k * C \tag{1.7}$$

where k is the apparent first-order metabolic rate constant. Drugs that are eliminated by first-order rate constant are said to obey first-order or linear kinetics. The elimination of drugs like phenytoin (*Tozer & Winter, 1992*) or salicylate (*Dromgoole & Furst, 1992*) cannot be described by first-order kinetics; the relative rate of elimination is slower at higher concentrations than at lower concentrations of drug in the plasma. Because their elimination decreases with increasing dose, their kinetics is said to be dose-dependent. Strictly speaking, however, Michaelis-Menten elimination is concentration-dependent rather than dose-dependent and means that clearance decreases with increasing drug concentration; however, drug clearance at a given drug concentration is the same whether a high or low dose is given (*Gibaldi, 1984*).

1.6.4.2 Dose and Time-Dependent Kinetics

Certain drugs display nonlinear pharmacokinetics that is not consistent with Michaelis-Menten kinetics. These drugs display dose-dependent or time-dependent pharmacokinetics rather than concentration-dependent pharmacokinetics. Displays of dose and time-dependent kinetics imply that clearance changes with dose rather than concentration. One plausible explanation is inactivation of liver enzyme(s), responsible for drug metabolism. This mechanism is not uncommon and has been observed with drugs such as diltiazem (*Hoglund & Nilsson, 1989*), lidocaine (Saville *et al.*, 1989) and verapamil (Schwartz *et al.*, 1985). It has been postulated that drugs with a tertiary amino group can inactivate *N*-dealkylating CYP isozymes by forming stable metabolic intermediates (Bast *et al.*, 1990). Mibefradil fulfills the structural requirements for such a

drug, since its chemical structure contains a tertiary amino function (Fig. 1.1). Another possible mechanism is product inhibition of drug metabolism which can lead to dose and time-dependent changes in elimination kinetics. It has been found that nordiazepam inhibits the metabolism of diazepam (Klotz *et al.*, 1976) and following multiple dosing, leads to a time-dependent reduction of diazepam elimination which is slower than elimination following a single dose (Klotz and Reimann, 1981).

Interestingly, it has been found recently in diltiazem studies using isolated perfused rat liver (*Hussain et al. 1994*) that mechanisms other than enzyme inactivation could be attributed to observed reduction in clearance. In that study it was concluded that the time-dependent kinetics of diltiazem in rats was mainly due to reversible tissue binding, suggesting that substrate binding to proteins in the liver can influence hepatic elimination.

1.6.5 Nonlinear Kinetics and Absolute Bioavailability

Absolute bioavailability is defined as the fraction of a dose reaching the general circulation. The following relationship describes this parameter:

$$F = \frac{D_{iv} * AUC_{po}}{D_{po} * AUC_{iv}} \tag{1.8}$$

and

$$F = F_a * F_H \tag{1.9}$$

where D_{iv} and D_{po} are intravenous and oral doses and AUC_{iv}, AUC_{po} are the corresponding areas under the plasma drug vs. time curve. As eq. 1.9 indicates, F value can be reduced by incomplete absorption and/or gut metabolism (F_a) and first-pass liver

metabolism (F_H). The AUC method (eq. 1.8) is based on the premise that clearance is constant during the elimination of the oral and intravenous doses (*Tozer & Rubin, 1988*). It is therefore difficult to assess the true bioavailability of drugs whose elimination kinetics changes with the route of administration.

1.6.6 Nonlinear Kinetics and Mibefradil

Currently, no data on the mechanisms responsible for the nonlinear pharmacokinetics of mibefradil in humans are available. An understanding of the causes of nonlinearity and the implications of such behaviour on concentration-time profiles is required if such drugs are to be used safely and efficaciously. Preliminary observations in humans would suggest (Table 1.1), that the absorption through the gut and liver first-pass effect are the two parameters worthwhile studying in greater detail. Detailed experimentation, otherwise inaccessible in humans, would therefore call for a suitable animal model.

1.7 Chronically Instrumented Conscious Dog Model

Dogs have proven to be a useful pharmacodynamic research tool during the development of mibefradil (*Orito et al. 1993*; *Mishra & Hermsmeyer, 1994*; *Vander Heide et al. 1994*) and a pharmacokinetic profile similar to that in humans, if proven, would unquestionably add to the validity of this species as a model of human pharmacokinetics and pharmacodynamics. We have recently developed a chronically instrumented,

conscious dog model (*O'Brien et al.*, 1991) which allows us to simultaneously monitor the time course of the drug in carotid artery, jugular, portal and hepatic veins with continuous measurement of hepatic blood flow. Therefore, the absorption through the gut and the rate of drug removal by the liver can be measured and quantified in a conscious animal. Therefore, the contribution of organs involved in elimination of mibefradil and their role in the nonlinear kinetic behaviour could be studied.

1.7.1 Hepatic Blood flow Measurements in a Conscious Dog Model

The accuracy and consistency of data recordings are of prime importance in experiments where methods of data collection and manipulation depend heavily upon physiological measurements. It is therefore essential that an experimental setting is thoroughly tested and validated before initiation of planned experiments.

Since its introduction into clinical research, the transit-time ultrasonic flowmeter has been successfully used to measure hepatic blood flow in humans and animals (*Doi et al. 1988*; *Transonic Systems. 1992*). Alternatively, indocyanine green (ICG) has been used widely as a noninvasive marker of hepatic blood flow and a liver function probe in humans and animals for the past thirty years (*Caesar et al. 1961*; *Kraft et al. 1991*; *Bonasch & Cornelius, 1964*). ICG, a tricarbocyanine dye, is an anionic compound; its use is based on the assumptions that it is highly extracted by the liver and systemic clearance will be equal to the liver blood flow. It would be therefore interesting to see how these two measurements, electronic and noninvasive, compare with one another.

1.7 Hypotheses

1. The pharmacokinetics of mibefradil in the dog are similar to those of the human and the dog would make a suitable animal model.

2. The pharmacokinetics of mibefradil after single oral doses are nonlinear due to a dose-dependent increase in absorption and/or reduction in elimination.

3. Pharmacokinetics of mibefradil after intravenous dosing are different from the pharmacokinetics after oral administration, thus affecting the accuracy of absolute bioavailability determination by the conventional approach.

4. An instrumented dog model will provide an estimate of the true bioavailability, using physiological measurements.

5. Pharmacokinetics after multiple oral doses cannot be predicted from the single dose parameters.

1.8 Objectives

1. To develop a suitable assay for measuring mibefradil in dog plasma and urine.

2. To evaluate the dog as an animal model of human mibefradil pharmacokinetics.

3. To evaluate and validate the most critical feature of the instrumented dog model, i.e. liver blood flow measurements, and compare them to a conventionally used, noninvasive marker of liver blood flow.

4. To explore potential mechanisms surrounding the nonlinear pharmacokinetics observed in humans.

5. To estimate absolute bioavailability of mibefradil in dogs using physiological measurements.

Table 1.1 Summary of pharmacokinetic parameters of mibefradil after intravenous and oral administration of single doses to healthy human volunteers (n=48, BW=74.4±7kg, age=25±2yrs). Data were extracted from *Welker et al., 1989*.

	Intravenous			***Oral***		
Parameter	**2.5 mg**	**10 mg**	**40 mg**	**10 mg**	**80 mg**	**320 mg**
Cl/F (ml/min)	288 (209-436)	321 (179-452)	241 (171-333)	1139 (581-1624)	369 (228-566)	162 (142-186)
V_{ss} (l)	278 (104-418)	241 (76-449)	213 (182-282)			
$T_{½}$ (h)	14.9 (8.4-24.6)	13.4 (7.3-20.2)	14.8 (13.2-17.5)	11.2 (4.5-22.2)	14.9 (14.0-15.9)	16.9 (12.5-20.9)
F				0.37 (0.15-0.90)	0.70 (0.42-1.22)	0.91 (0.90-0.92)

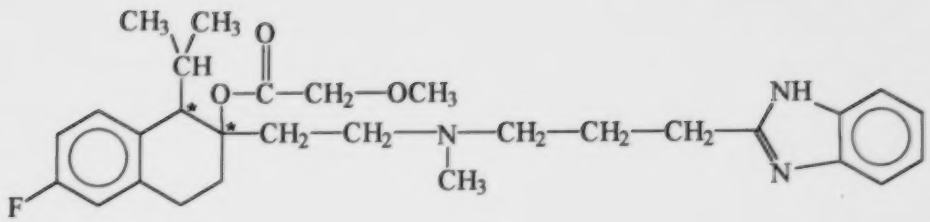

Figure 1.1 Structure of mibefradil (* denotes the chiral center), (1S,2S)-2-[2-[[3-(2-benzimidazolyl)propyl]methylamino]ethyl]-6-fluoro-1,2,3,4-tetrahydro-1-isopropyl-2-naphthyl methoxyacetate.

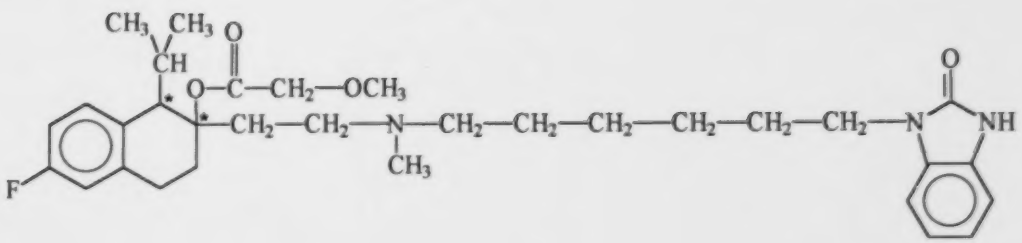

Figure 1.2 Structure of internal standard (* denotes the chiral center). Internal standard is the S,S-isomer.

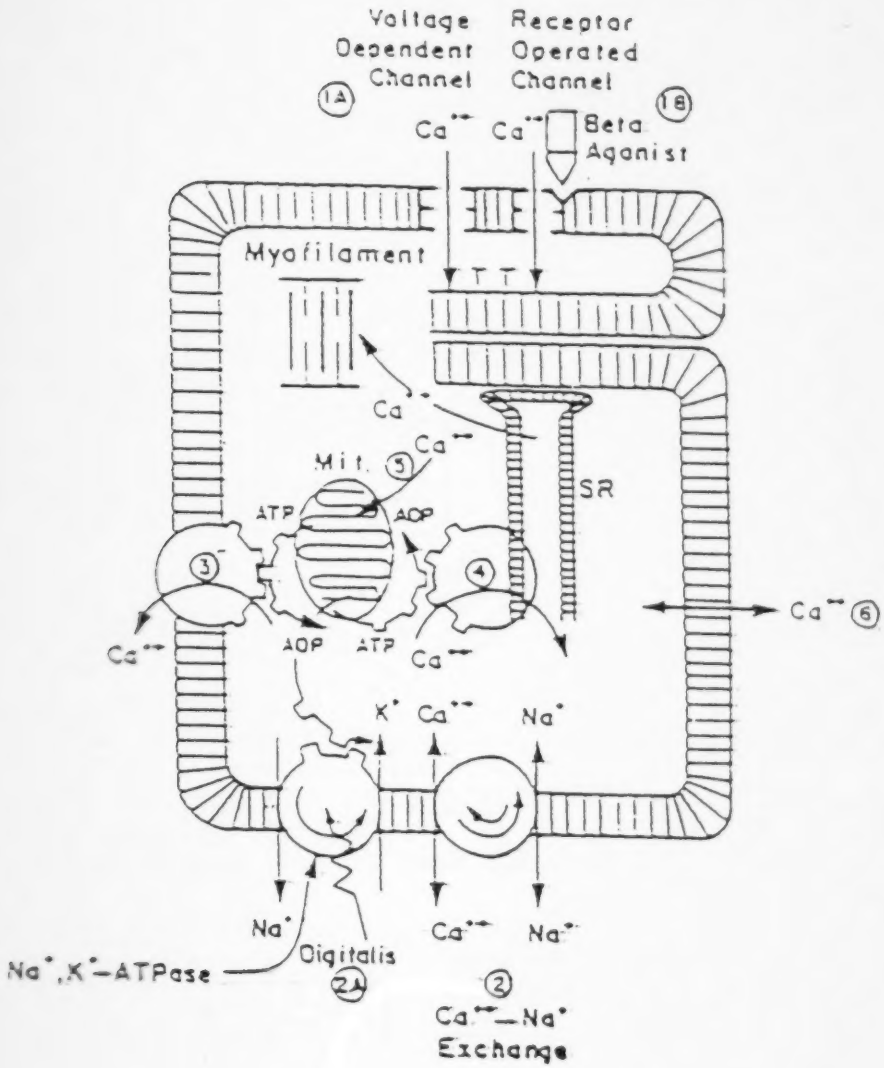

Figure 1.2 The regulation of Ca^{2+} in myocardium. TT denotes transverse tubule, SR sarcoplasmic reticulum and Mit. mitochondrion. Numbers in circles denote the mechanisms affecting intracellular Ca^{2+} (*Braunwald, 1982*).

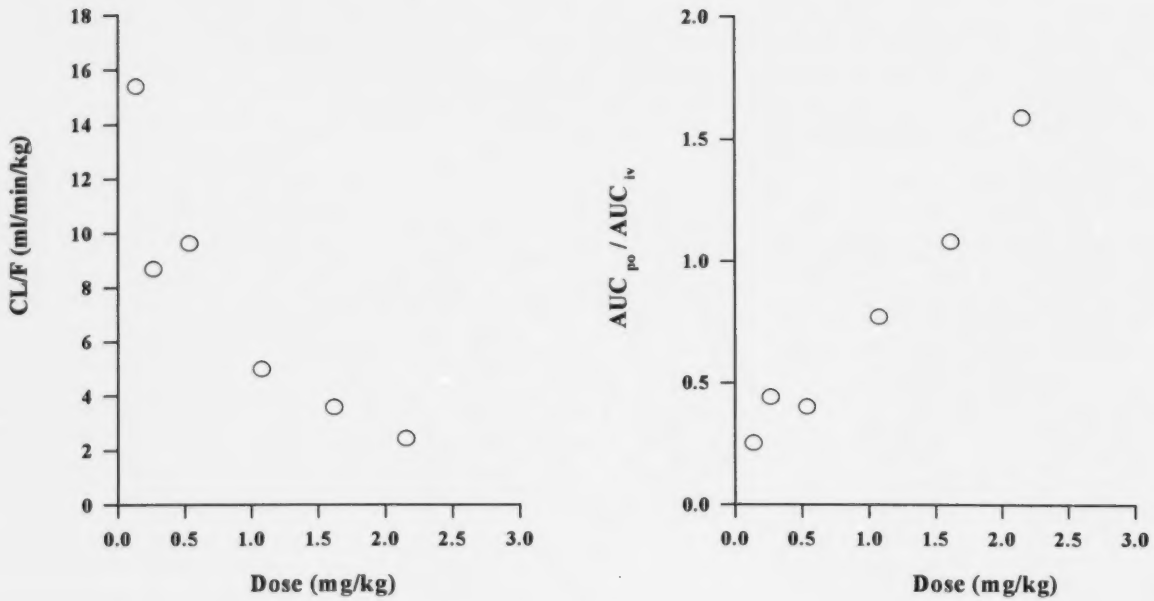

Figure 1.3 Relationship between the oral clearance (left panel), dose normalized plasma AUC_{po}/AUC_{iv} ratios (right panel) and the dose after single oral doses to humans (for clarity, doses were normalized for body weight). Adapted from *Welker et al. 1989*.

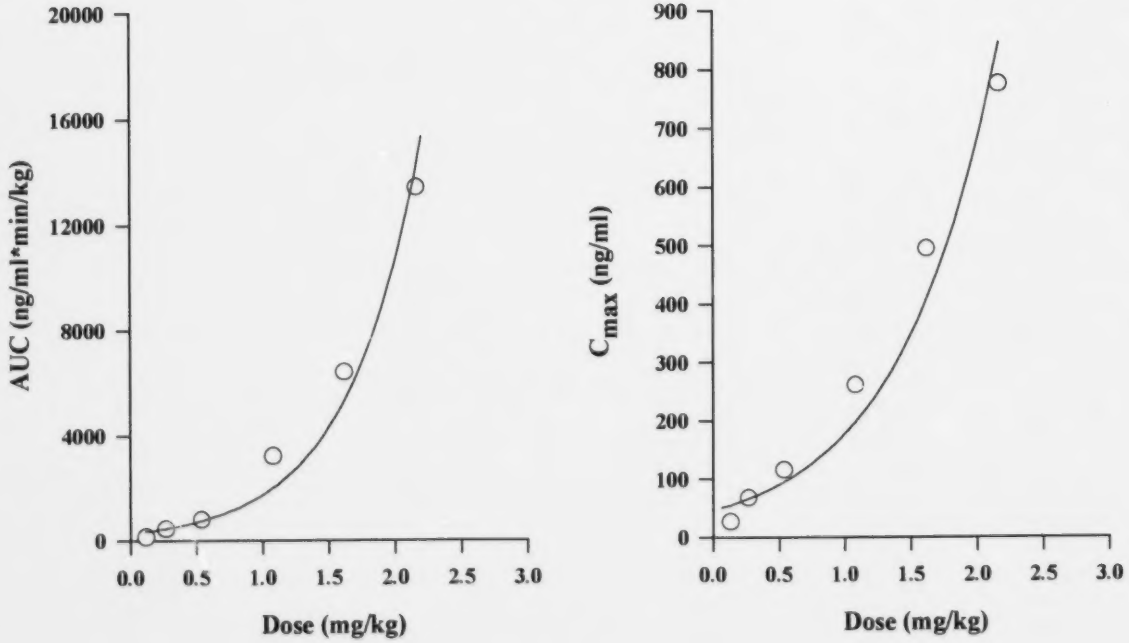

Figure 1.4 Relationship between the AUC (left panel), C_{max} (right panel) and the dose after single oral doses to humans (for clarity. doses were normalized for body weight). Adapted from Welker et al. 1989.

2. EXPERIMENTAL SECTION[1]

2.1 Chemicals and Assay Procedures

2.1.1 HPLC Assay of Mibefradil in Dog Plasma and Urine

The hydrochloride salts of mibefradil and internal standard (Ro 40-6792) were kindly supplied by Hoffmann-La Roche (Basel, Switzerland). The structures of mibefradil and internal standard are shown in Figures 1.1 and 1.2, respectively. Solvents, acetonitrile and tertiary-butyl-methyl ether, were HPLC grade (Fischer Scientific, Montreal, Canada). Other chemicals such as KH_2PO_4, $KHCO_3$ (BDH, Toronto, Canada) and the sodium salt of pentanesulphonic acid (Sigma, St. Louis, MO, USA) were analytical grade.

2.1.1.1 Standard solutions

Standard stock solutions of mibefradil were prepared in deionized water to provide final concentrations of 5 and 10 μg/ml base equivalent. The concentration of the internal

---

[1] A version of this and subsequent chapters has been published/submitted for publication. Skerjanec, A., O'Brien, D. W., and Tam, Y. K. Hepatic blood flow measurements and indocyanine green kinetics in a chronic dog model. *Pharmaceutical Research* 11:1511-1515, 1994. Skerjanec, A. and Tam, Y. K. HPLC analysis of mibefradil in dog plasma and urine. *Journal of Chromatography:Biomedial Applications* 1995, in press. Skerjanec, A., Tawfik, S., and Tam, Y. K. Nonlinear pharmacokinetics of mibefradil: an evaluation of the dog as an animal model. *Journal of Pharmaceutical Sciences*, submitted. Skerjanec, A., Tawfik, S., and Tam, Y. K. Mechanisms of Dose and Time Dependent Kinetics of Mibefradil in Chronically Instrumented Dogs. *Journal of Pharmacology and Experimental Therapeutics*, submitted.

standard solution was 8 μg/ml base in deionized water. Drug-free dog plasma and urine samples were spiked with the appropriate stock solution of mibefradil. Serial dilutions with the appropriate biological matrix gave standard concentrations ranging from 10 to 500 ng/ml in plasma and 10 to 200 ng/ml in urine. Stock solutions of mibefradil and internal standard were prepared every 3 months and stored at -25°C; working solutions were kept at 4°C for a period of a month.

2.1.1.2 Sample preparation

Saturated solution of $KHCO_3$ (0.5 ml) and 50 μl of internal standard solution were added to the 0.5 ml aliquots of plasma and 0.2 ml aliquots of urine. Aliquots (0.25 ml) of plasma samples exceeding the standard curve range were diluted with blank plasma to a volume of 0.5 ml. Each sample was extracted with 2ml of tertiary-butyl-methyl ether by vortexing for 30 sec and centrifuged at 1000 g for 3 minutes. The lower water phase was frozen on acetone/dry ice bath and the organic phase was transferred into clean tubes (Kimax®, Kimble, IL, USA) and evaporated under vacuum (Savant Instruments, Farmingdale, NY, USA). The residue was reconstituted in 200 μl of mobile phase and 30-130 μl of this solution was injected onto the HPLC system. The extraction efficiency was found to be higher than 90% for mibefradil.

2.1.1.3 Instrumentation and chromatographic conditions

The HPLC system consisted of a SIL 9A automatic injector (Shimadzu), a Model 501 pump, a Model 470 scanning fluorescence detector and IBM-compatible PC with a Baseline 810 data processing software (Waters, Mississauga, Canada). The detector was set at λ_{EX} = 270nm and λ_{EM} = 300nm and chromatographic separation was achieved on a reversed-phase column (Merck, LiChrospher, C-18, RP Select-B). The mobile phase composition was a mixture of acetonitrile and aqueous solution (38:62 v/v). The aqueous solution contains 0.0393 M KH_2PO_4 and 0.0082 M sodiumpentanesulphonate. Mobile phase was pumped at a flow rate of 2 ml/min.

2.1.1.4 Calibration curves and assay validation

Calibration curves were generated by weighted (1/c) least-squares regression of the analyte/internal standard peak-height ratio vs. the concentration of the analyte. Assay was validated using quality control (QC) samples prepared by an authorized person in the laboratory. The concentration of these QC samples covered the range of the calibration curve. Intra-assay accuracy and precision were assessed from replicate analyses (n=3) of spiked plasma at four different concentrations (10, 30, 200 and 500 ng/ml) on the same day. Three replicates were performed for urine at the concentrations of 10, 30 and 200 ng/ml. Inter-assay validation for plasma and urine was performed on three separate occasions.

2.1.2 Indocyanine Green Studies

Indocyanine Green (Cardio-Green®) was purchased from Becton Dickinson, USA. ICG standards and plasma samples were measured spectrophotometrically at 805nm (Becton Dickinson). The assay performance was tested against the validated manufacturer's procedure, encompassing a range of ICG plasma concentrations from 1 to 12 mg/l. Accuracy and precision of the assay fell within a 5% interval of the reference procedure values, with a standard curve $y = 0.26x+0.016$, where optical density is plotted on y-axis and corresponding ICG plasma concentration on x-axis (*Becton Dickinson*). During ICG studies, an aliquot of ICG injection solution was stabilized with dog blank plasma and used for standard curve preparation, performed immediately after the experiment.

Since the commercially available ICG contains a 1 to 3% of decomposition product, the conventional spectrophotometric assay lacks specificity. However, the decomposition product does not interfere with an assay within the first 20 min of the ICG time course in the plasma due to the relatively higher concentrations of ICG in plasma (*Rappaport and Thiessen, 1982*; *Heintz et al., 1986*; *Ott et al., 1993*). Therefore, the ICG plasma profiles should be accurately measured within a 15 min time interval after the intravenous bolus administration of ICG and this time interval is sufficient to characterize the ICG disposition in the body.

2.2 Instrumentation

2.2.1 Blood Flow Measurements

For blood flow measurements, transit-time ultrasonic flow probes and a flow meter (Model T201, Transonic Systems, Ithaca, NY) were used. Blood flow was recorded on an IBM-compatible PC using the P-Option software (Transonic Systems). Flow probes were factory tested and precalibrated. Additionally, we performed our bench testing before the surgery and after the probes were recovered from the dogs. Calibration ranges encompassed 0-400 ml/min and 0-2000 ml/min interval for hepatic artery and portal vein, respectively. All tests gave results within 10% of the reading from a timed collection method. For experimental blood flow measurements, moving average of 10 sec (n=10) was used to filter blood flow measurements (*Oppenheim & Schafer, 1975*).

2.3 Surgery, Postoperative Care and Catheter Maintenance

Surgical protocol was approved by the Health Sciences and Animal Welfare Committee at the University of Alberta. A detailed description of the surgical procedure was published recently (O'Brien *et al.*, 1991). Briefly, four catheters were inserted into jugular, portal, hepatic veins and carotid artery and two blood flow probes placed around the portal vein and hepatic artery. For indocyanine green noninstrumented studies, a single jugular vein catheter was inserted, while jugular vein and carotid artery catheters were inserted for mibefradil pharmacokinetic studies using noninstrumented dogs. After surgery, dogs were fitted with jackets with side pockets (Alice King Chatham Medical

Arts, Los Angeles, CA) to protect the catheters. The animal was allowed to heal for at least 2 weeks before experiments were initiated. The subjects were fed canned dog food (Dr. Ballard, Friskies Pet Care, Don Mills, Canada), combined with Tuffy's chunks (Star Kist Foods, Willowdale, Canada) and had free access to water. Skin interfaces were cleaned daily with H_2O_2 and sprayed with dilute gentamicin spray (gentamicin sulphate 1.1 mg/ml, Shering, Canada Inc., Point Claire, Quebec). The catheters were flushed every 3 days by removing the heparin locks, instilling 0.9% sodium chloride, followed by ACD solution to fill the catheter dead space. The ACD solution consisted of 0.4% anhydrous citric acid, 1.32% sodium citrate (dihydrate), 1.47% dextrose (mono H_2O), and 1.5% of 37% formaldehyde and was left for 5 min to sterilize the catheters' lumens and then removed. The catheters were flushed with sterile saline and then filled with heparin solution (1000 U/ml during first 5 days and 10000 U/ml thereafter). A sling that provided gentle restraint and support to the animal was used during the procedures. The dog was able to stand freely in the sling or be supported along its entire ventral surface, thus taking the weight off its legs.

2.3 Design of Animal Experiments

Random source, mixed breed female dogs were selected for the study. Physiological parameters such as body weight, blood and liver clinical biochemistry tests were monitored in all dogs from the arrival date at animal facilities and throughout the investigations. Hematocrit, white blood cell count, red blood cell count and hemoglobin

were monitored weekly. Clinical biochemistry tests such as AGT (serum alanine glutamine transferase), AST (serum alanine sulphotransferase), ALP (alkaline phosphatase), BUN (blood urea nitrogen) and creatinine were performed before and after the surgical procedures.

2.3.1 Blood Flow Measurements and Indocyanine Green Kinetics

Seven dogs (3m, 4f, BW = 21 ± 1.8 kg, Hct = 0.39 ± 0.05) were used in these experiments. Three dogs underwent the ICG study prior to surgery to examine potential effects of implanted catheters on the kinetics of ICG. Three dogs were used (crossover study) to study the effect of increased hepatic blood flow on ICG kinetics. Standard dog ration (1 can of Dr. Ballard, 630g) was given to induce liver blood flow increase. Plateau effect was reached after 30 minutes and remained stable throughout the experiment.

On the day of an experiment, the dog was brought to the laboratory at 9 a.m. having been fasted overnight and placed in a sling frame that both restrained and supported the animal gently. The dog was able to stand freely in the sling or be supported along its entire ventral surface, thus taking the weight off its legs. All dogs were accustomed to this procedure during the recovery period and catheter maintenance. In all experiments, 0.5mg/kg of ICG was administered as a bolus injection into the left cephalic vein, and blood samples were collected at 0, 2.5, 5, 7.5, 10, 12.5 and 15 minutes. Fed dogs received the bolus dose 30 minutes after the food intake. Fed and fasted dog experiments were separated by a week. ICG plasma concentration-time profiles in all four

catheters and liver blood flows were recorded simultaneously and blood flow rates based on ICG kinetics and electronic measurements were examined.

2.3.2 Mibefradil Pharmacokinetic Studies

Two groups of female dogs weighing between 19 and 24 kg were selected for the studies. First group consisted of three and second group consisted of four dogs dogs.

2.3.2.1 Experimental protocol

1mg/kg intravenous and 1, 3 and 6 mg/kg oral doses were independently administered to the first group of three dogs (noninstrumented) according to a randomized complete block design, where dogs represented blocks and the four treatments were randomly assigned to each block. An identical protocol was applied to the instrumented (group 2, 4 dogs) dog study except a multiple oral dose treatment (3 mg/kg q12h, 8 days) was added. At least one week washout period was allowed between the treatments. This washout period is sufficient to allow for complete elimination of the drug from the body and for the recovery of CYP-450 enzymes that could be potentially affected by mibefradil treatment (*Gasser et al., 1982*). Dogs were fasted overnight, 24 hours prior to the experiment, but allowed water *ad libitum*. Food and water were withheld during the first 6 hours of the experimental period. During the noninstrumented experiments, dogs were kept in the metabolic cages which allowed continuous urine sample collection.

2.3.2.2 Intravenous Dosing - Noninstrumented Dogs

The left cephalic vein was cannulated using an 21-gauge cannula to which a three-way stop-cock was attached. A 1mg/kg base equivalent of mibefradil dihydrochloride salt powder, dissolved in 17ml of sterile 0.9% NaCl solution was infused through the cannula at a constant rate over 10 minutes. Each dog was returned to its metabolic cage 30 min after the completion of infusion. Blood samples (3 ml) were drawn from the jugular vein and carotid artery catheters at 0, 5, 10, 15, 20, 30, 45, 60, 90, 120 min and 3, 6, 12, 24, 36 hours and urine samples were collected from the beginning of the infusion and up to 48 hours after. Heparin lock (10 U/ml) was used throughout all experiments to maintain patency of the blood sampling catheters. Before a blood sample was taken, the heparin in the catheter was removed. Based on our previous experience with basic drugs such as lidocaine, propranolol and diltiazem, the residual effect of heparin has no effect on the plasma protein binding. Blood samples were collected in polypropylene tubes containing 0.1M EDTA (25 µl/ml blood). After centrifugation, plasma was transferred to separate tubes and stored at -20^{0}C until analysis. Urine samples were collected once or twice daily, volumes recorded and aliquots stored in polypropylene tubes at -20^{0}C until analysis.

2.3.2.3 Intravenous Dosing - Instrumented Dogs

The description is identical to the procedure in section *2.3.2.2*, except for the following modifications:

1. All four dogs received a 1 mg/kg treatment.

2. Blood samples (3 ml) were drawn from all four catheters at 0, 5, 10, 15, 20, 30, 45, 60, 90, 120 min and 3, 6, 12, 24, 36 hours after the beginning of infusion.

3. Mibefradil plasma concentration-time profiles from all four catheters and hepatic blood flow rates were recorded simultaneously.

4. Dogs were returned to their cages 3 hours after the initiation of experiment. They were brought back into the lab for each subsequent sampling point and immediately returned after collection of blood samples and recording of flow-rates.

5. Urine samples were not collected.

2.3.2.4 Oral Dosing - Noninstrumented Dogs

Appropriate amounts of mibefradil dihydrochloride salt powder that provided 1, 3, and 6mg/kg of mibefradil base equivalent was weighed into gelatine capsules. After administration of the capsule, containing the assigned dose, 15ml of tap water was administered orally by means of a syringe. Blood samples (3 ml) were drawn from the jugular vein catheter at 0, 5, 15, 30, 45, 60, 90, 120 min and 3, 6, 12, 24, 36, 48, 60 and 72 hours and urine samples were collected from the beginning of the study and up to 96 hours after dosing. Blood and urine samples were processed as described in section *2.3.2.2.*

2.3.2.5 Oral Dosing - Instrumented Dogs

The procedure was identical to noninstrumented dog studies, except for:

1. A multiple oral dose treatment was added: 3 mg/kg base equivalent twice a day over a period of 8 days.
2. Blood samples (3 ml) were drawn from all four catheters at 0, 5, 15, 30, 45, 60, 90, 120 min and 3, 6, 12, 24, 36, 48, 60 and 72 hours for single dose studies and at 0, 5, 15, 30, 45, 60, 90, 120 min and 3, 6, 12 hours after the last dose of the 8 days dosing schedule.
3. Mibefradil plasma concentration-time profiles in blood from all four catheters and hepatic blood flow rates were recorded simultaneously.
4. Dogs were returned to their cages 3 hours after the initiation of experiment. They were brought back into the lab for each subsequent sampling point and immediately returned after collection of blood samples and determination of flow-rates.
5. Urine samples were not collected.

2.3.2.6 Plasma Protein Binding Studies in Dogs

In vitro protein binding of mibefradil was extensively studied in human and dog plasma pools using ultrafiltration method (*Brand & Meyer, 1988*) We have performed a set of plasma protein binding studies using ultrafiltration method at 37^{0}C. Dog plasma was collected before and after the surgery and binding studies were performed on both sets of

plasma. Due to the extensive binding of mibefradil to the plasma proteins, a single 2000 ng/ml concentration (n=3) was used which was close to the value used in the original report (1400 ng/ml, *Brand & Meyer, 1988*).

2.4 Data Analysis

2.4.1 Pharmacokinetic Analysis

2.4.1.1 Blood Flow Measurements and Indocyanine Green Kinetics

ICG plasma versus time data were subjected to nonlinear regression analysis using PCNONLIN (*Metzler & Weiner, 1992*). A one compartment open model was adequate to describe all data sets. Based on these calculations, the following parameters were obtained:

$$Cl_S = \frac{Dose}{AUC} \tag{2.1}$$

$$Cl_B = \frac{Dose}{AUC * (1 - Hct)} \tag{2.2}$$

$$t_{½} = \frac{\ln 2}{K_e} \tag{2.3}$$

$$V_d = \frac{C_o}{Dose} \tag{2.4}$$

where Cl_S Cl_B, $t_{½}$, and V_d are ICG jugular vein based plasma systemic clearance, hematocrit adjusted blood systemic clearance, half-life and plasma volume of distribution,

respectively. Eq. 2.2 assumes that no distribution into red blood cells occurs and literature on ICG supports this assumption (*Daneshmend et al., 1981*). ICG hepatic extraction ratio was calculated as follows:

$$E_H = \frac{flux_{in} - flux_{out}}{flux_{in}} \tag{2.5}$$

where fluxes were computed on a point-by-point basis according to eq. 3.6 and 3.7:

$$flux_{in} = \frac{Q_{HA} * C_{CA} + Q_{PV} * C_{PV}}{(1 - Hct)} \tag{2.6}$$

$$flux_{out} = \frac{(Q_{HA} + Q_{PV}) * C_{HV}}{(1 - Hct)} \tag{2.7}$$

with Q_{HA} and Q_{PV} as blood flow rate of hepatic artery and portal vein, and C_{CA}, C_{PV}, C_{HV} are carotid artery, portal vein and hepatic vein plasma ICG concentrations, respectively.

ICG lung extraction was estimated on a point-by-point basis as follows:

$$E_L = \frac{C_{JV} - C_{CA}}{C_{CA}} \tag{2.8}$$

where C_{JV} and C_{CA} are jugular vein and carotid artery ICG plasma concentrations. Individual values of E_H (eq. 2.5) and E_L (eq. 2.8) were pooled and averaged over the 15 min period. Hepatic blood flow based on ICG kinetics was calculated according to the following equation:

$$Q = \frac{CL_B}{E_H} \tag{2.9}$$

where E_H and CL_B are calculated as described above.

2.4.1.2 Mibefradil - Noninstrumented Dogs

Pharmacokinetic parameters were obtained using established non-compartmental analysis (*Gibaldi & Perrier, 1982*). Area under the plasma concentration-time curve (AUC) and the area under the first moment curve (AUMC) from time zero to the last sample time point were calculated using the Lagrange method (*Rocci, Jr. & Jusko, 1983*) and the terminal extrapolated portion of the curve was estimated by dividing the concentration at the last sampling time point by the slope of the terminal elimination phase. Systemic and oral clearance, volume of distribution at steady-state and half-life of the terminal phase of mibefradil were calculated using standard formulae (*Gibaldi & Perrier, 1982*). Maximum drug concentration, C_{max}, and its corresponding time point, T_{max}, were read from the raw data of plasma concentration vs. time profile. Due to an apparent nonlinearity, as described later in the results section, the relative ratio between dose normalized AUC_{po}/AUC_{iv} rather than absolute bioavailability term was used. All kinetic parameters were normalized for dose and body weight, when appropriate.

2.4.1.3 Mibefradil - Instrumented Dogs

Pharmacokinetic analysis of jugular vein profiles was identical to that used for noninstrumented dogs, which is described in section *2.4.1.2*.

2.4.1.4 Mibefradil - Instrumented Dogs: Measurement of Physiological Kinetic Parameters

Plasma profiles in individual blood vessels, combined with electronically measured portal vein and hepatic artery blood flows were used to quanify processes such as the extent of gut absorption, F_a, absolute bioavailability, F, hepatic extraction, E_H, and hepatic availability, F_H, hepatic clearance, Cl_H, systemic clearance, Cl_S and volume of distribution, V_β, of mibefradil in a conscious animal. The following equations were used to calculate the parameters:

$$F_a = \frac{Amount\ absorbed}{Dose} \tag{2.10}$$

Absolute bioavailability of mibefradil was estimated using equation 2.11:

$$F = F_a * F_H \tag{2.11}$$

The amount of drug absorbed from the gut (equation 2.12) was calculated by integrating the absorption fluxes from the time point of the first appearance of the drug into the portal system up to the point when portal vein and carotid artery plasma profiles overlapped. The criteria for selecting the last point were set as follows: when a difference in drug concentration less than 15% between the two blood vessels was detected for three consecutive time points, the first point was selected as the time when absorption was considered complete.

$$Amount\ absorbed = \int_{t_1}^{t_2} Absorption\ flux\ dT = \int_{t_1}^{t_2} Q_{PV} * (C_{PV} - C_{CA})\ dt \qquad (2.12)$$

where Q_{PV}, C_{PV} and C_{CA} are portal vein blood flow rate, portal vein and carotid artery plasma concentrations, respectively. E_H and F_H were calculated using eq. 2.5 and 2.13:

$$E_H = \frac{flux_{in} - flux_{out}}{flux_{in}} \qquad (2.5)$$

$$F_H = 1 - E_H \qquad (2.13)$$

The corresponding fluxes were calculated according to eq. 2.14 an 2.15. Fluxes were integrated from the beginning of the study up to the last measured plasma concentration point:

$$flux_{in} = \int_{t_1}^{t_2} (C_{PV} * Q_{PV} + C_{CA} * Q_{HA})\ dt \qquad (2.14)$$

$$flux_{out} = \int_{t_1}^{t_2} [C_{HV} * (Q_{PV} + Q_{HA})]\ dt \qquad (2.15)$$

where Q_{HA} is the blood flow rate of hepatic artery, and C_{HV} is the hepatic vein plasma mibefradil concentration. Average systemic clearance was calculated using equation 2.16:

$$Cl_s = \frac{F * D}{AUC} \tag{2.16}$$

where D is the intravenous or oral dose of mibefradil, F is obtained from equation 2.10 and AUC is the corresponding area under the plasma concentration vs. time curve from 0 to ∞. Average hepatic clearance, Cl_H, from the time of the first appearance of mibefradil in the body up to the last measured plasma concentration point was calculated using equations 2.17, 2.18 and 2.19:

$$Cl_H = \frac{\int_{t_1}^{t_2} Cl_H^{mid} * AUC_{dt}\ \mathrm{dt}}{AUC} \tag{2.17}$$

$$Cl_H^{mid} = \frac{Cl_H^{t_1} + Cl_H^{t_2}}{2} \tag{2.18}$$

$$Cl_H^t = Q_H^t * E_H^t \tag{2.19}$$

where Cl_H^{mid} is hepatic clearance at the mid-point of the time interval between the sampling points, AUC_{dT} is the area under the mibefradil plasma concentration vs. time curve within the time interval between the two sampling points and AUC is the area under the mibefradil plasma concentration vs. time curve from 0 to ∞. Cl_H was calculated from the time of the first appearance of the drug in the body up to the last measured point. Q_H^t is hepatic blood flow rate (Q_{PV}+Q_{HA}) and E_H^t is hepatic extraction ratio obtained from equation 2.5, calculated on a point-by-point basis.

Volume of distribution in terminal disposition phase, V_β, after intravenous and oral doses of mibefradil was calculated as follows:

$$V_\beta = \frac{Cl_H^{post}}{\beta} \qquad (2.20)$$

where Cl_H^{post} is hepatic clearance calculated by using equation 2.17 in post-absorption, post-distribution phase and β is terminal elimination phase rate constant. Plasma concentrations were used in all calculations since blood to plasma ratio of mibefradil equals unity.

2.4.2 Statistical Analysis

2.4.2.1 Blood Flow Measurements and Indocyanine Green Kinetics

Student's paired t-test at the significance level of P = 0.05 was performed. All values are reported as mean ± S.D, except for electronically measured blood flows, where the values are reported as mean ± SEM.

2.4.2.2 Mibefradil Pharmacokinetics in Noninstrumented and Instrumented Dogs

All pharmacokinetic parameters were evaluated according to a randomized complete block design, where dogs were assigned to blocks and treatments randomly assigned to each block. All parameters, undergoing statistical evaluation, were first tested for normal distribution (Wilk-Shapiro test) and variance homogeneity (Levene test), (*Zar,*

1984; SAS for Windows. 1994). Parameters, deviating from normality were subjected to Friedman's nonparametric ANOVA (*Milliken & Johnson, 1984; SPSS for Windows. 1994*). If F statistics indicated significant diferences among the treatment groups ($P<0.05$), Duncan's multiple range test was used to determine which treatment group was different. Paired t-test was used to compare time to maximum concentration (T_{max}) between portal and hepatic vein catheters (Table 3.7). All values are reported as mean ± SD, except for electronically measured blood flow rates, where the values are reported as mean ± SEM.

3. RESULTS

3.1 HPLC Assay of Mibefradil in Dog Plasma and Urine

Representative chromatograms are shown in Figures 3.1 and 3.2. The retention time of mibefradil was 10.7 min while the internal standard eluted at 12.2 minutes. Using 0.5 ml of plasma and 0.2 ml of urine, calibration curves with concentrations ranging from 10-500 ng/ml for plasma and 10-200 ng/ml for urine were linear ($r^2 > 0.99$). The regression equations in plasma and urine were $y = 190x + 1.4$ and $y = 188x + 1.1$, respectively where y-axis represent a detector response and x-axis a corresponding mibefradil concentration. The detection limit for mibefradil was 0.5 ng/ml for both biological media. Dilution of urine samples was not required since the urinary excretion of mibefradil in dogs is less than a 1 % of the dose after intravenous and oral administration.

Assay performance during routine analysis was evaluated using quality control samples resulting in similar accuracy and precision for both biological media (Table 3.1).

3.2 Blood Flow Measurements and Indocyanine Green Kinetics

The results suggest that surgical instrumentation has no effect on ICG disposition kinetics (Table 3.2). Pharmacokinetic parameters, ICG and electronically measured blood flow values from chronically instrumented dogs that underwent ICG treatment are summarized in Table 3.3. Plasma ICG concentration followed a monoexponential decline with time during the first 15 min (Fig. 3.3A) and the half-life of 8.9 ± 1.6 min. Estimated volume of distribution closely approximated plasma volume in the dog (V_d = 45.7 ± 5.9 ml/kg). Systemic blood clearance was low compared to the electronically measured hepatic blood flow rate (Cl_B = 5.9 ± 1.1 ml/min/kg vs. Q = 27.8 ± 9.1 ml/min/kg) and extraction ratios estimated using ICG fluxes from the inlet and the outlet of the liver were consistent with the clearance values, suggesting that ICG is not highly extracted by dog livers (E_H = 0.15 ± 0.05). Extrahepatic uptake of ICG, as demonstrated by extraction across the lungs, was substantially lower than that of the liver (E_L = 0.06 ± 0.06) and the values varied among dogs. Electronically measured blood flow values in individual blood vessels during experiments were 6.6 ± 2.1 ml/min/kg in hepatic artery and 21.2 ± 2.5 ml/min/kg in portal vein (Fig. 3.3B). Blood flow, estimated from ICG systemic blood clearance and liver extraction ratio was 42.8 ± 16 ml/min/kg, and overestimated electronically measured blood flows by an average of 56%.

Results from fasted and fed studies are summarized in Table 3.4. Food intake did not influence the pharmacokinetics of ICG and all measured kinetic and ICG based blood flow parameters remained unchanged between the two experiments. However, food intake resulted in an overall increase in electronically measured liver blood flow (30% increase), while blood flow rate estimated using ICG data remained unaltered.

3.3 Mibefradil Pharmacokinetics in Noninstrumented Dogs

3.3.1 Intravenous Study

Intravenous mibefradil plasma concentration vs. time profiles are shown in Figure 3.4A. Mean systemic plasma clearance, volume of distribution at steady-state and half-life were as follows: Cl_s = 18.4 ± 1.2 ml/min/kg, V_{ss} = 9.7 ± 3.8 l/kg and $T_{½}$ = 9.5 ± 3.4 h (Table 3.5). Blood to plasma ratio of mibefradil equaled unity within the range of concentration vs. time profiles, observed in our studies. Urinary excretion of mibefradil after an intravenous dose was negligible. Pharmacokinetic parameters calculated from carotid artery plasma profiles were quantitatively similar to those obtained from the jugular vein. The difference is less than 6%, indicating a lack of arterio-venous difference.

3.3.2 Oral Study

The plasma concentration vs. time profiles of the single oral doses of mibefradil in the four dogs are depicted in Figure 3.4B. AUC_{po} and C_{max} increased in a nonlinear

fashion with an increase in dose (Figure 3.5). Consequently, oral plasma clearance decreased with an increase in dose, from 101.8 ± 18.8 ml/min/kg at 1mg/kg dose to 21.7 ± 4.3 ml/min/kg at 6mg/kg dose while the dose normalized AUC ratios between oral and intravenous treatments increased from 0.18 ± 0.03 to 0.87 ± 0.21, respectively (Table 3.5). Both parameters at 1, 3 and the 6 mg/kg dose were statistically different between each other ($P<0.05$). Mean half-life values did not change significantly with an increasing oral dose (Table 3.5). Similar to intravenous studies, urinary excretion of mibefradil after oral doses was not quantifiable.

3.4 Mibefradil Pharmacokinetics in Instrumented Dogs

3.4.1 Jugular vein intravenous and oral data

Intravenous mibefradil plasma concentration vs. time profiles are presented in Figure 3.6A. Data from this treatment show that mibefradil systemic clearance is high and distribution extensive (Table 3.6), an observation consistent with the results obtained from the study in noninstrumented dogs (Skerjanec *et al.*, 1995). The plasma concentration vs. time profiles of single and multiple oral doses of mibefradil in four dogs are depicted in Figure 3.6B. Oral clearance decreased with increasing doses, suggesting nonlinear disposition. At the highest dose, 6 mg/kg, Cl_o values were approximately 1/2 of that of 1 mg/kg dose, while the dose normalized AUC_{po}/AUC_{iv} ratios increased approximately two and a half-fold within the same dose range (Table 3.6). Continuous oral dosing for 8 days with the 3 mg/kg twice a day brought about a further decrease in Cl_o value which was

approximately 1/3 the value of a single 6 mg/kg dose. This reduction in Cl_o was accompanied by a two-fold increase in dose normalized AUC_{po}/AUC_{iv} ratios and both parameters were significantly different from the corresponding parameters after the single dose treatments ($P<0.05$). The $t_{½}$ values were not sensitive to a change in Cl_o values and $t_{½}$ did not change significantly when compared across the range of doses studied (Table 3.6). The accuracy of $t_{½}$ determination during multiple doses however, can be erroneous because the time interval for the estimation is less than one half-life.

3.4.2 Pharmacokinetic analysis based on measurement of physiological kinetic parameters

Figure 3.7 is a set of representative plasma mibefradil concentration vs. time profiles in a dog that received a single 3 mg/kg oral dose. Portal vein carried the highest concentration of mibefradil during the absorption phase and was similar to that of carotid artery at and after 360 minutes, indicating completion of absorption. Absorption was complete within 360 minutes in all animals who received the remaining oral treatments. The fraction of mibefradil absorbed through the gut was independent of the dose administered ($F_a \approx 0.60$), suggesting that absorption is either incomplete or this drug undergoes first-pass gut metabolism (Table 3.7). Using the absorption data obtained from equation 2.11, a graph of logarithm of the % amount of drug that remained to be absorbed vs. time was used to described the kinetics of absorption from the gut after single and multiple doses (Fig. 3.8). Monoexponential decline would suggest that absorption is a

linear, first-order process, with an exponent corresponding to the absorption rate constant, K_a. This rate constant was calculated using a nonlinear, curve-fitting method (*Metzler & Weiner, 1992*). Results revealed that the rate of gut absorption is best described by two first-order processes, one of which is responsible for >90% of an absorbed dose (Table 3.7); no difference in K_a values among the four oral treatment groups was found ($P>0.05$). T_{max} values in the portal vein are not significantly different after all oral dose treatments ($P>0.05$, Table 3.7). The absorption parameters suggest that gut absorption kinetics are insensitive to dose and duration of treatment. An absorption lag-time of less than 10 min was found in the portal circulation (Fig. 3.8), suggesting rapid dissolution and absorption of mibefradil after dosing. A significant time lag between peak portal and hepatic vein concentrations ($T_{max, PV}$ vs. $T_{max, HV}$) was observed for all but the 1 mg/kg dose ($P<0.05$, Table 3.7), suggesting that equilibration process in the hepatic tissue is not instantaneous. Volume of distribution, V_β, indicates a trend of reduction with increasing oral doses, and V_β values after 6 mg/kg single and multiple 3 mg/kg oral doses decreased significantly when compared to that of intravenous treatment ($P<0.05$, Table 3.7). These observations were consistent in all the subjects studied and suggest that binding of mibefradil to tissues is capacity-limited.

Examination of hepatic extraction revealed that initial E_H values are high, probably due to simultaneous distribution and elimination of the drug in the liver (Fig. 3.9). E_H values were the highest after intravenous dosing; a mean value of 0.71 places mibefradil in a highly extracted drug category (Table 3.8). The time course of E_H values was stable during and after intravenous infusion in contrast to that after oral administration, where E_H

values dropped rapidly and reached a lowest point at approximately 120 min before rebounding to a more stable value. The reduction of E_H values after oral administration was a dose and time dependent process. The magnitude of decrease is about 40% from 1 to 6 mg/kg single dose and about 50% between the single and multiple 3 mg/kg dose (Table 3.8). E_H values after multiple doses were significantly different from all but 6 mg/kg dose ($P<0.05$). Hepatic blood flow rate increased in a dose-dependent manner during the absorption phase. This increase is attributed to an increase in hepatic arterial blood flow rate (Fig 3.9, upper panel). The increase was approximately 30% after a single 1 mg/kg dose and 60% after a 6 mg/kg dose (Fig. 3.10, lower panel). This change in hepatic blood was transient, reached its maximum at approximately 60 min after the administration of the single oral doses and 20 min after intravenous and multiple oral doses, and began to decline towards a predose level thereafter.

Average Cl_H values were similar to Cl_S values (Table 3.8), suggesting that liver is the main organ for eliminating mibefradil. After oral administration, the time course of hepatic clearance (Fig. 3.11) paralleled that of hepatic extraction ratio (Fig. 3.9); the decrease of CL_H values was dose related and was the lowest during peak absorption. Overall Cl_H reached the lowest values after the highest single and after multiple oral doses ($P>0.05$, Table 3.8).

Since the absorption from the gut was dose independent, absolute bioavailability followed a reverse trend of E_H; reduction of E_H led to an increase in F. Consistent with this trend, F increased by 60% from 1 to 6 mg/kg single dose and doubled when the 3

mg/kg multiple dose was compared to its single dose counterpart (Table 3.8). F after multiple doses was significantly different from all but the 6 mg/kg dose ($P<0.05$).

3.5 Plasma Protein Binding Studies in Dogs

Ultrafiltration method using dog plasma from our studies produced results, consistent with the previously published report (*Brand & Meyer, 1988*). Mibefradil is higly bound to the plasma proteins in dogs. The free fraction value in dogs at 2000 ng/ml is 1.06 ± 0.08 % in plasma collected before the surgery and 1.03 ± 0.06% in plasma obtained from the dogs 4-weeks after the surgery. These results suggest that surgical intervention did not alter the extent of mibefradil plasma protein binding in dogs.

Table 3.1 Accuracy and precision of the assay for mibefradil in plasma (PL) and urine (UR).

Concentration added (ng/ml)	Intra-day (n=3)				Inter-day (n=3)			
	Accuracy (%)		Precision CV (%)		Accuracy (%)		Precision CV (%)	
	PL	UR	PL	UR	PL	UR	PL	UR
10.0	105.7	103.9	2.1	3.1	109.1	95.8	5.5	6.0
30.0	94.7	101.3	6.1	4.6	94.7	99.0	6.1	5.0
200.0	103.9	96.0	3.1	4.0	96.0	97.0	3.2	6.1
500.0	104.5		2.1		103.0		1.2	

Table 3.2 Comparison of indocyanine green pharmacokinetic parameters before and after the instrumentation.

	instrumented			*noninstrumented*		
DOG	Cl_S *(ml/min/kg)*	$t_{½}$ *(min)*	V_d *(ml/kg)*	Cl_S *(ml/min/kg)*	$t_{½}$ *(min)*	V_d *(ml/kg)*
#3	3.5	8.8	43.9	3.5	7.9	39.9
#4	3.4	11.2	55.1	2.8	11.3	46.4
#6	3.9	7.3	40.3	4.3	6.9	42.6
AVG	3.6	9.1	46.4	3.5	8.7	42.9
STD	0.3	1.9	7.7	0.7	2.3	3.7

Table 3.3 Pharmacokinetic parameters for chronically instrumented dogs that underwent the ICG treatment. Electronically measured blood flows in hepatic artery (Q_{HA}), portal vein (Q_{PV}), sum of arterial and portal blood flow (Q), ICG based hepatic blood flow (Q_{ICG}) and ratio between ICG estimated and electronically measured hepatic blood flows.

DOG	Cl_B *(ml/min/kg)*	$t_{½}$ *(min)*	V_d *(ml/kg)*	E_H	E_L	Q_{HA} *(ml/min/kg)*	Q_{PV} *(ml/min/kg)*	Q *(ml/min/kg)*	Q_{ICG} *(ml/min/kg)*	Q_{ICG}/Q
#1	6.6	7.4	46.2	0.14	0.07	18.3	20.8	39.1	46.7	1.19
#2	7.2	8.4	51.2	0.14	0.03	5.1	34.8	39.9	51.9	1.30
#3	5.5	8.8	43.9	0.25	0.04	2.8	15.0	17.8	22.4	1.26
#4	6.6	11.2	55.1	0.11	0.02	4.8	20.2	25.0	58.6	2.34
#5	3.7	11.1	38.3	0.14	0.05	1.8	16.0	17.8	26.7	1.50
#6	6.1	7.3	40.3	0.20	0.00	4.5	20.2	24.7	30.9	1.25
#7	5.7	8.4	44.9	0.09	0.18	8.5	21.5	30.0	62.2	2.07
AVG	5.9	8.9	45.7	0.15	0.06	6.6	21.2	27.8	42.8	1.56
STD	1.1	1.6	5.9	0.05	0.06	*2.1	*2.5	*9.1	16.0	0.46

* mean ± SEM

Table 3.4 Food effect on electronically and ICG measured hepatic blood flow (Q and Q_{ICG}) and ICG disposition characteristics.

fasted						
DOG	Cl_B ***(ml/min/kg)***	$t_{½}$ ***(min)***	V_d ***(ml/kg)***	E_H	Q^* ***(ml/min/kg***	Q_{ICG} ***(ml/min/kg***
#4	6.5	11.2	55.1	0.11	25.0	58.4
#6	6.0	7.3	40.3	0.20	24.7	30.5
#7	5.7	8.4	44.9	0.09	30.0	61.9
AVG	6.1	9.0	46.8	0.13	26.6	50.2
STD	0.4	2.0	7.6	0.06	3.0	17.2

fed						
DOG	Cl_B ***(ml/min/kg)***	$t_{½}$ ***(min)***	V_d ***(ml/kg)***	E_H	Q^* ***(ml/min/kg***	Q_{ICG} ***(ml/min/kg***
#4	5.1	11.6	48.1	0.09	33.7	54.8
#6	5.6	8.6	42.7	0.11	34.9	51.2
#7	4.4	10.0	41.1	0.09	35.1	51.1
AVG	5.0	10.1	43.9	0.10	34.6	52.4
STD	0.6	1.5	3.7	0.01	0.8	2.1

* $P<0.05$.

Table 3.5 Mibefradil pharmacokinetic parameters in four dogs after single intravenous doses of 1 mg/kg and three oral doses of 1, 3 and 6 mg/kg.

Parameter	intravenous	oral		
	1mg/kg	1mg/kg	3mg/kg	6mg/kg
AUC (ng/ml*min/kg)	2603±280	439±79	3905±333	12461±2940
Cl_s (ml/min/kg)	18.4±1.2			
Cl_o (ml/min/kg)		101.8±18.8 [a]	45.4±5.51 [a]	21.7±4.3 [a]
V_{ss} (l/kg)	9.7±3.8			
$t_{1/2}$ (h)	9.5±3.4	10.6±1.5	12.1±2.1	13.4±3.5
C_{max} (ng/ml)	715.3±187.8	19.4±11.7 [b]	119.5±18 [b]	481.2±71.8 [b]
T_{max} (min)	10	45±15	100±35	70±17
AUC_{po}/AUC_{iv} [#]		0.18±0.03 [a]	0.41±0.05 [a]	0.87±0.21 [a]

[a] significantly different from each other at p=0.05
[b] significantly different from each other at p=0.05, when normalized for the dose and body weight
[#] dose normalized ratios

Table 3.6 Mibefradil jugular vein based pharmacokinetic parameters in four instrumented dogs after single intravenous doses of 1 mg/kg, three single oral doses of 1, 3 and 6 mg/kg and multiple doses of 3 mg/kg, q12h for 8 days.

	intravenous	oral			
Parameter	1mg/kg	1mg/kg	3mg/kg	6mg/kg	3mg/kg, q12h
AUC (ng/ml*min/kg)	2525±493	771±275	2612±875	13256±4854	13594±5974
Cl_s (ml/min/kg)	18.5±4.4				
Cl_o (ml/min/kg)		71.3±24.9	57.0±11.0	35.8±11.5 [a]	12.3±6.6 [b]
V_{ss} (l/kg)	10.4±1.4				
$t_{1/2}$ (h)	10.6±1.4	13.1±3.3	11.0±3.4	14.3±1.5	18.8.2±7.9
AUC_{po}/AUC_{iv} [#]		0.36±0.41	0.34±0.11	0.92±0.56	1.90±1.00 [b]

[a] significantly different from 1 mg/kg single oral doses ($P<0.05$)
[b] significantly different from 1,3 and 6 mg/kg single oral doses ($P<0.05$)
[#] dose normalized

Table 3.7 Mibefradil pharmacokinetic parameters in four instrumented dogs after single intravenous doses of 1 mg/kg, three single oral doses of 1, 3 and 6 mg/kg and multiple doses of 3 mg/kg twice a day for 8 days. Fraction of the dose absorbed through the gut (F_a), absorption rate constant (K_a) and % total amount absorbed at a rate constant corresponding to K_a. Time at which a maximum concentration occurs (T_{max}) is reported for hepatic (HV), portal (PV) and jugular vein (JV) catheters.

	intravenous	oral			
Parameter	1mg/kg	1mg/kg	3mg/kg	6mg/kg	3mg/kg twice a day
F_a		0.61±0.12	0.56±0.20	0.64±0.11	0.67±0.25
K_a (min^{-1})		0.028±0.016	0.018±0.013	0.035±0.015	0.027±0.016
% total amount absorbed through K_a		87.1±9.1	93.4±10.3	93.5±7.2	95.6±6.7
$T_{max,PV}$ (min)	10	52±47	41±14	38±36	30±12
$T_{max,HV}$ (min)	10	64±39	98±15 [a]	79±33 [a]	64±19 [a]
V_β (l/kg)	19.3±5.0	17.4±12.3	16.8±8.0	11.1±2.6 [b]	11.5±4.2 [b]

[a] significantly different from corresponding portal vein catheter at P=0.05 (t-test)
[b] significantly different from intravenous dose at P=0.05

Table 3.8 Mibefradil pharmacokinetic parameters in four instrumented dogs after single intravenous doses of 1 mg/kg, three single oral doses of 1, 3 and 6 mg/kg and multiple doses of 3 mg/kg. Calculations are based on electronically measured hepatic blood flows and plasma profiles in carotid artery, portal and hepatic vein (see section *2.4.1.4* for detailed description).

	intravenous	oral			
Parameter	1mg/kg	1mg/kg	3mg/kg	6mg/kg	3mg/kg, q12h
E_H	0.71±0.11	0.60±0.24	0.54±0.13	0.38±0.29 [b]	0.27±0.15 [a]
CL_H (ml/min/kg)	20.1±5.5	16.7±5.4	15.7±1.4	10.6±2.9 [c]	8.2±2.9 [a]
CL_S (ml/min/kg)	18.5±4.4	15.6±9.7	17.2±5.1	9.0±1.3 [c]	7.0±3.5 [a]
F_H	0.29±0.11	0.40±0.24	0.46±0.13	0.62±0.29 [b]	0.73±0.15 [a]
F		0.25±0.18	0.24±0.01	0.40±0.22	0.48±0.14 [d]

[a] significantly different from 1 mg/kg intravenous and 1 and 3 mg/kg single oral doses at P=0.05
[b] significantly different from 1 mg/kg intravenous and 1 mg/kg single oral doses at P=0.05
[c] significantly different from 1 mg/kg intravenous and 3 mg/kg single oral dose at P=0.05
[d] significantly different from 3 mg/kg single oral dose at P=0.05

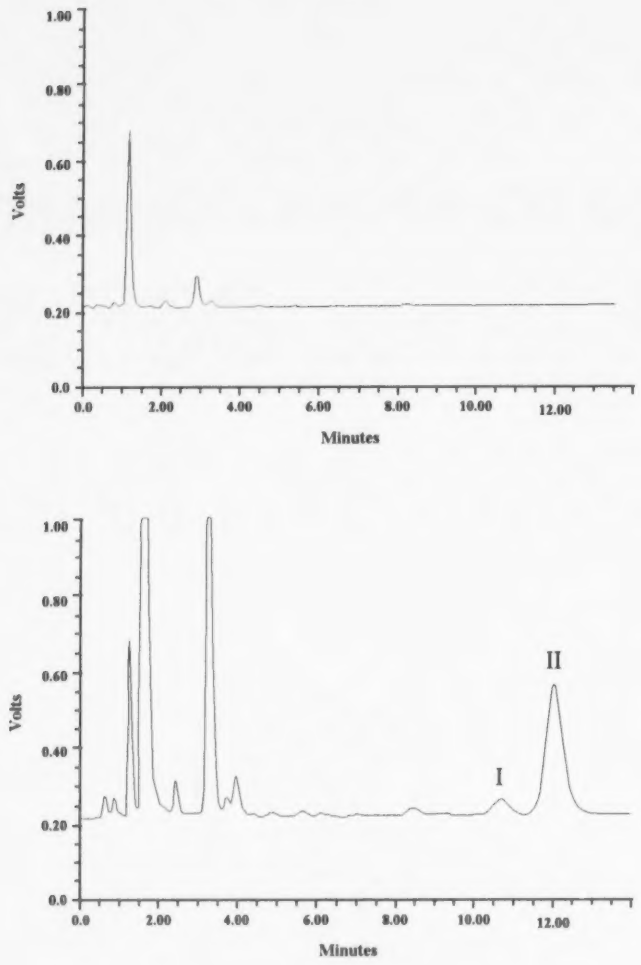

Figure 3.1 Representative chromatograms of blank dog plasma (upper panel) and dog plasma sample taken at 36h after 3 mg/kg single oral dose of mibefradil (I) (lower panel). The concentration of mibefradil corresponds to 12 ng/ml. II denotes internal standard.

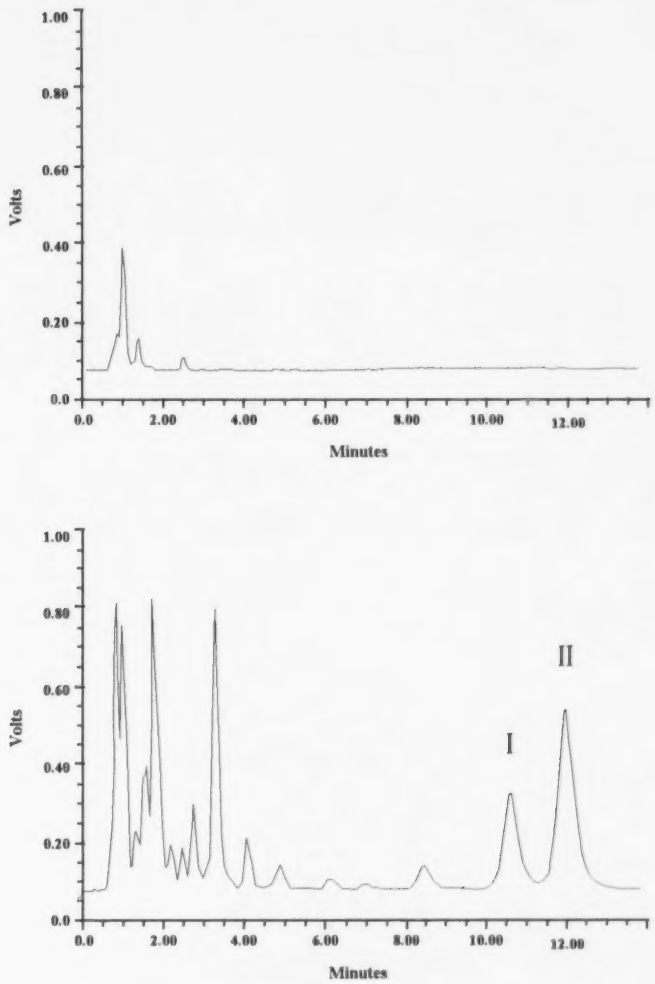

Figure 3.2 Representative chromatograms of blank dog urine (upper panel) and dog urine sample collected between 12-24 hours after a single oral dose of 6 mg/kg of mibefradil (I) (lower panel). The concentration of mibefradil corresponds to 64 ng/ml. II denotes internal standard.

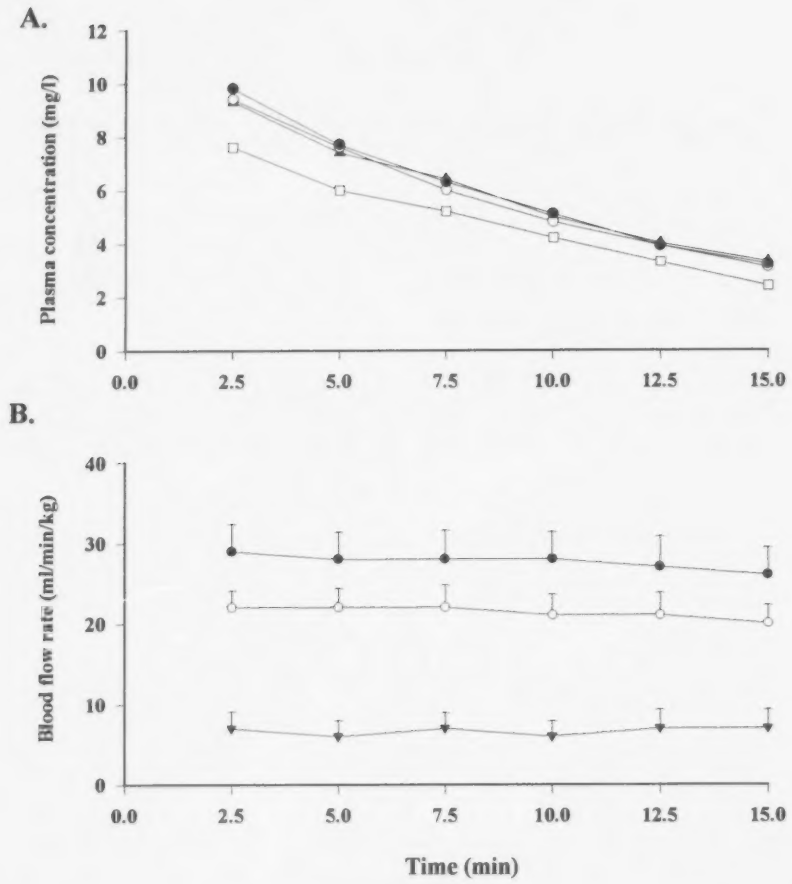

Figure 3.3 (A) ICG plasma vs. time profile in a representative dog; jugular vein (●), carotid artery (o), portal vein (▲), hepatic vein (□). (B) Electronically measured blood flow rates during the ICG experiments in dogs; total liver flow (●), portal vein flow (o), hepatic artery flow (▼). Each data point represents the mean (±SEM) of seven dogs.

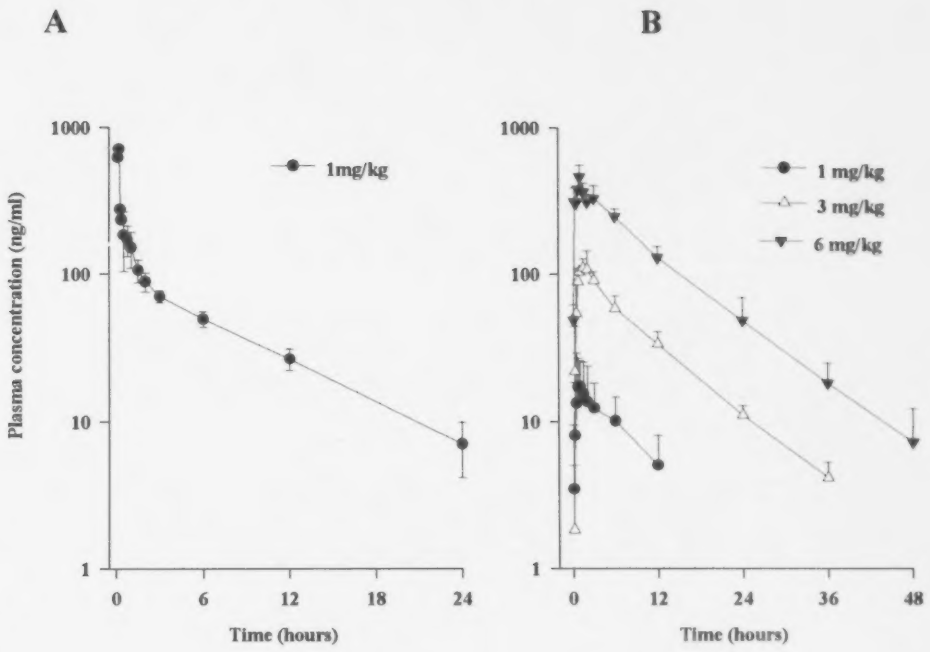

Figure 3.4 Plasma concentration vs. time profile of mibefradil in 3 dogs after (**A**) intravenous (•) and (**B**) oral administration.

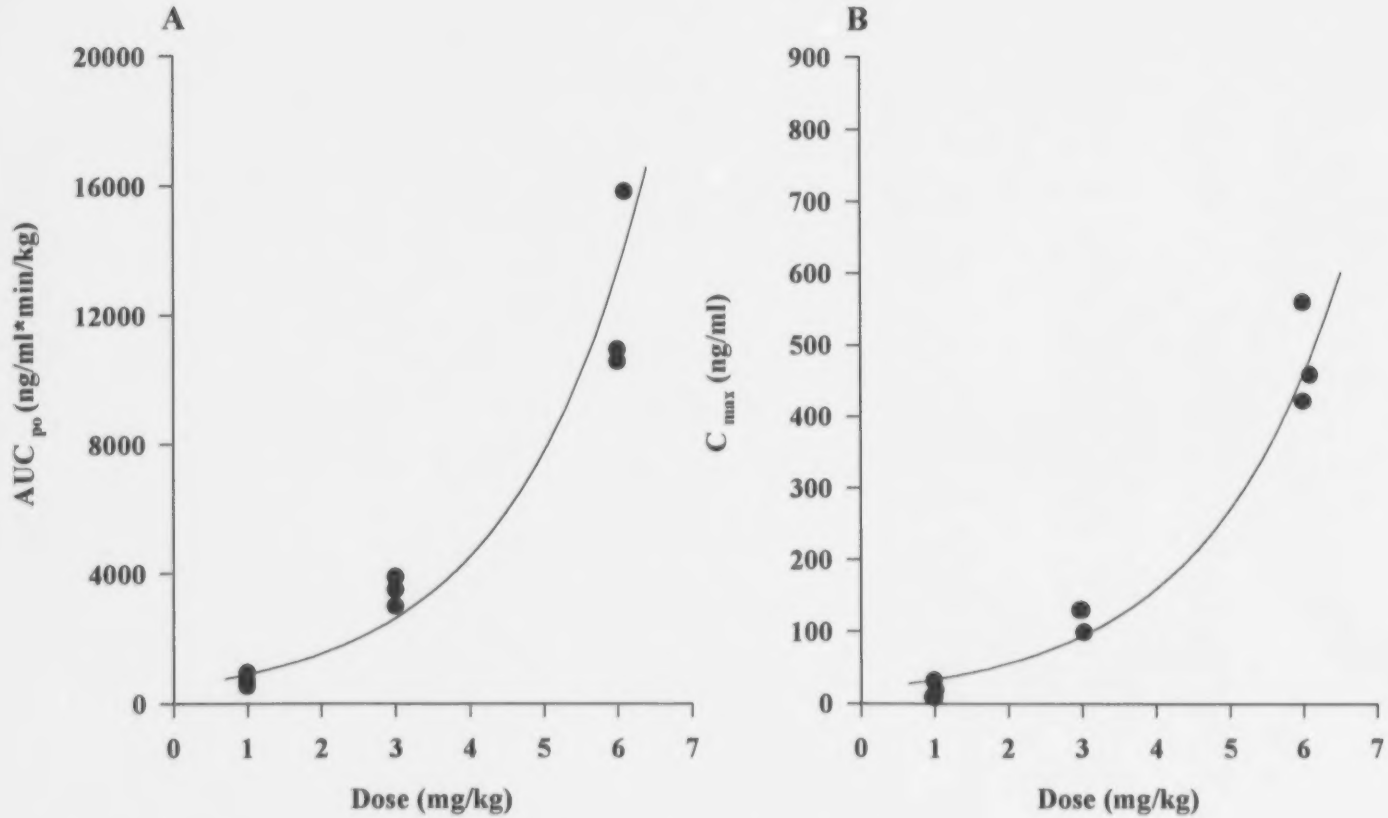

Figure 3.5 Relationship between the **(A)** AUC, **(B)** C_{max}, and the dose after single oral doses to 3 dogs.

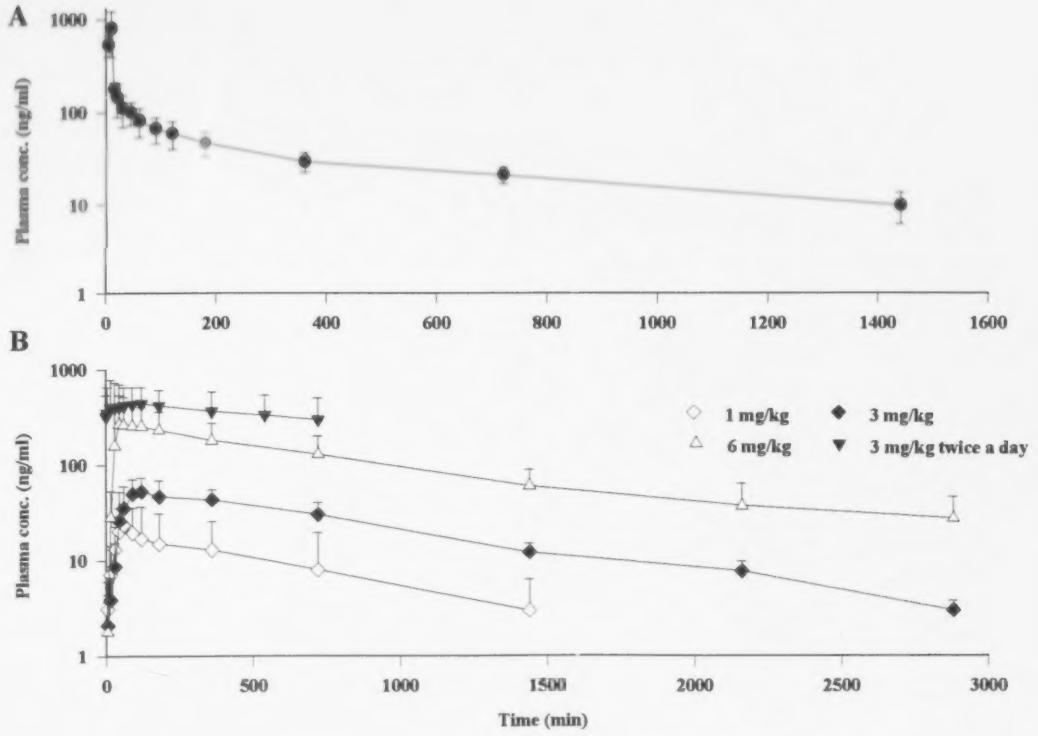

Figure 3.6 Plasma concentration vs. time profile of mibefradil in four dogs after **(A)** intravenous administration of 1 mg/kg dose and **(B)** oral administration of 1, 3, 6 mg/kg single and 3 mg/kg multiple doses to 4 dogs.

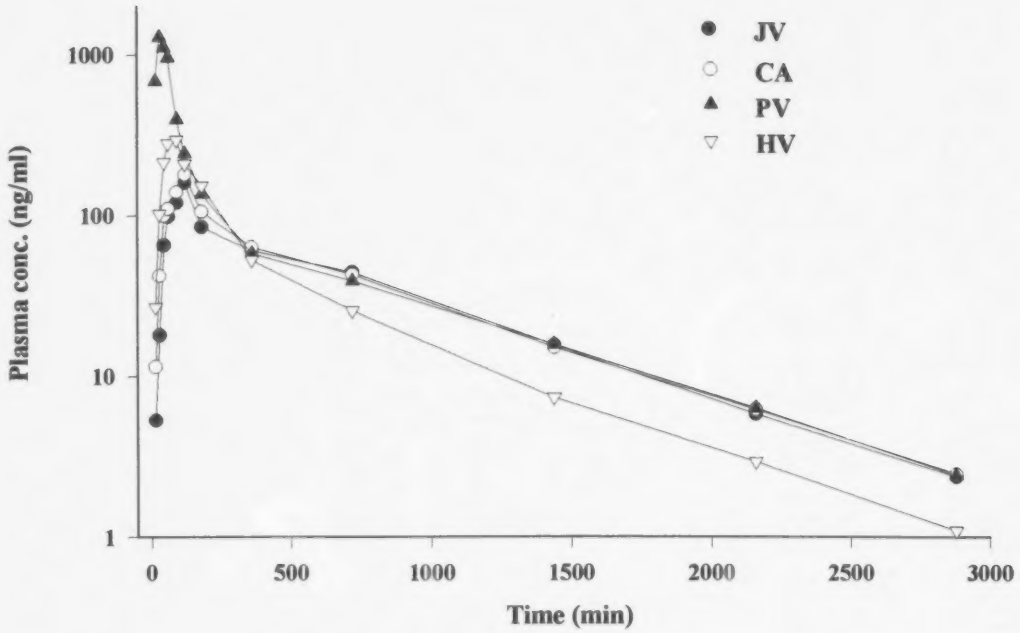

Figure 3.7 Plasma concentration vs. time profile of mibefradil in four catheters after 3 mg/kg single oral dose in a representative dog. (JV) Jugular vein, (CA) Carotid artery, (PV) Portal vein, (HV) Hepatic vein.

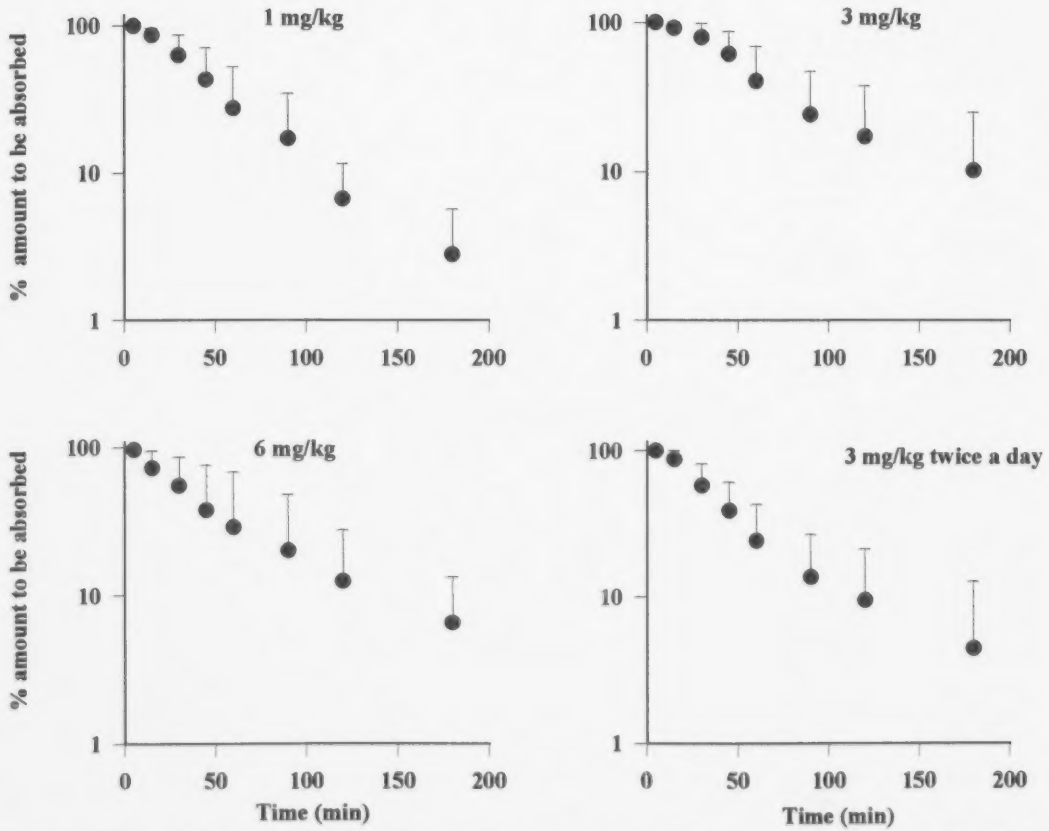

Figure 3.8 Plot of % amount of mibefradil to be absorbed vs. time after oral administration of single 1, 3 and 6 mg/kg doses and multiple 3 mg/kg doses.

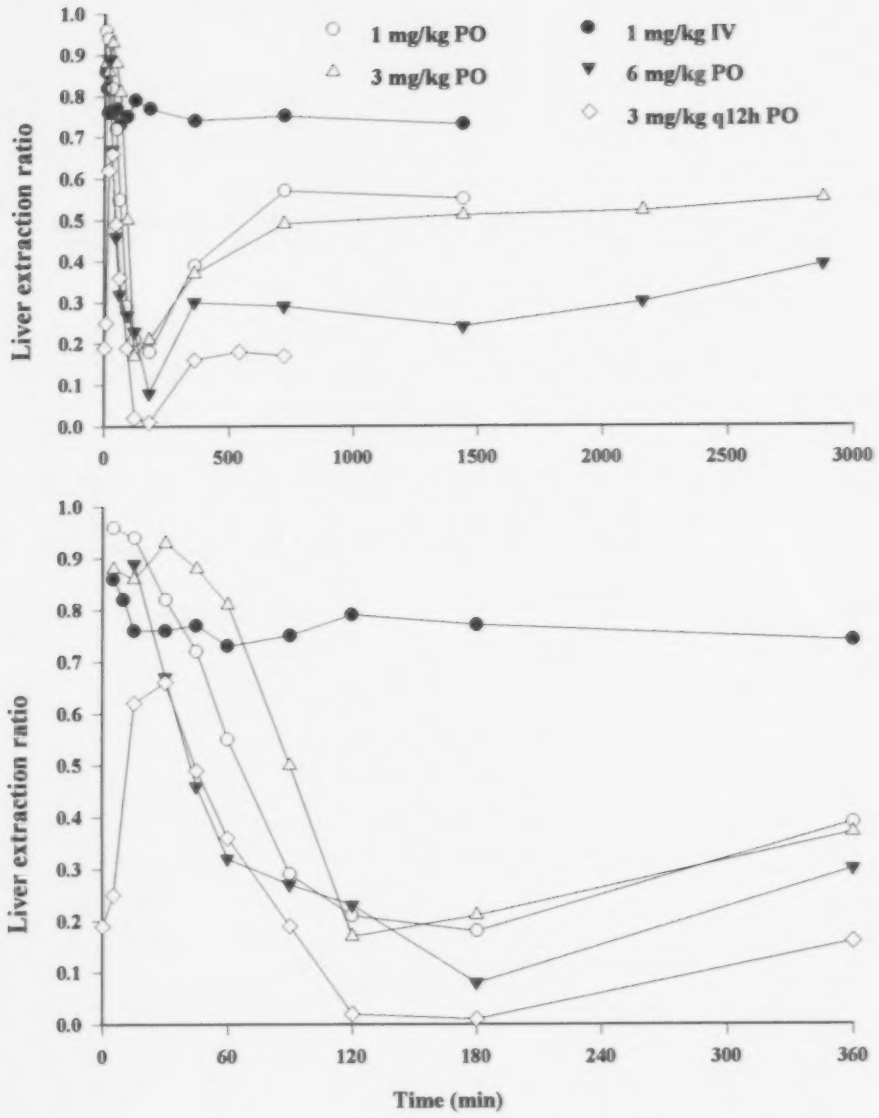

Figure 3.9 Time course of the mean hepatic extraction ratio after 1 mg/kg intravenous and oral administration of 1, 3 and 6 mg/kg single and 3 mg/kg multiple oral doses in four dogs. Upper panel comprises the entire time course of the drug in the body, lower panel represents the first 360 min time profile. (For clarity, only mean values are depicted.)

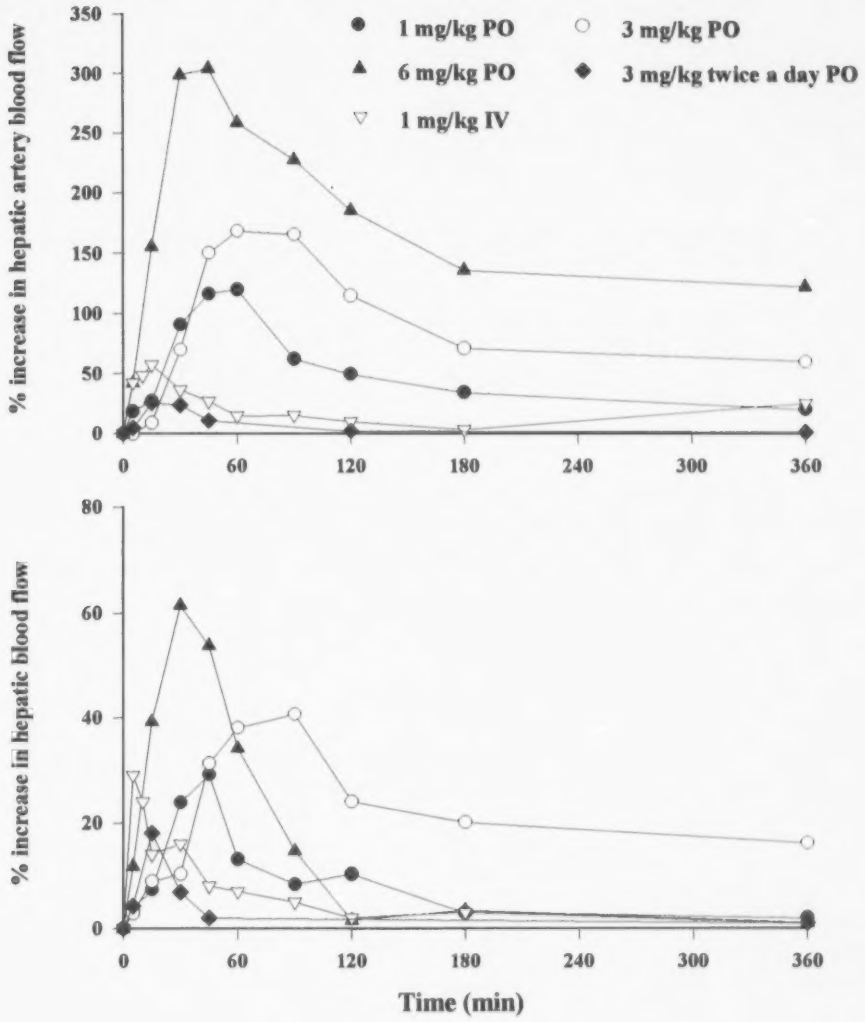
1 mg/kg PO
3 mg/kg PO
6 mg/kg PO
3 mg/kg twice a day PO
1 mg/kg IV
% increase in hepatic artery blood flow
% increase in hepatic blood flow
Time (min)

Figure 3.10 Time course of the average increase (%) in hepatic arterial blood flow (upper panel) and average increase (%) in hepatic blood flow (lower panel) during the first 360 min after 1 mg/kg intravenous and oral administration of 1, 3 and 6 mg/kg single and 3 mg/kg multiple oral doses in four dogs. (For ciarity, only mean values are depicted.)

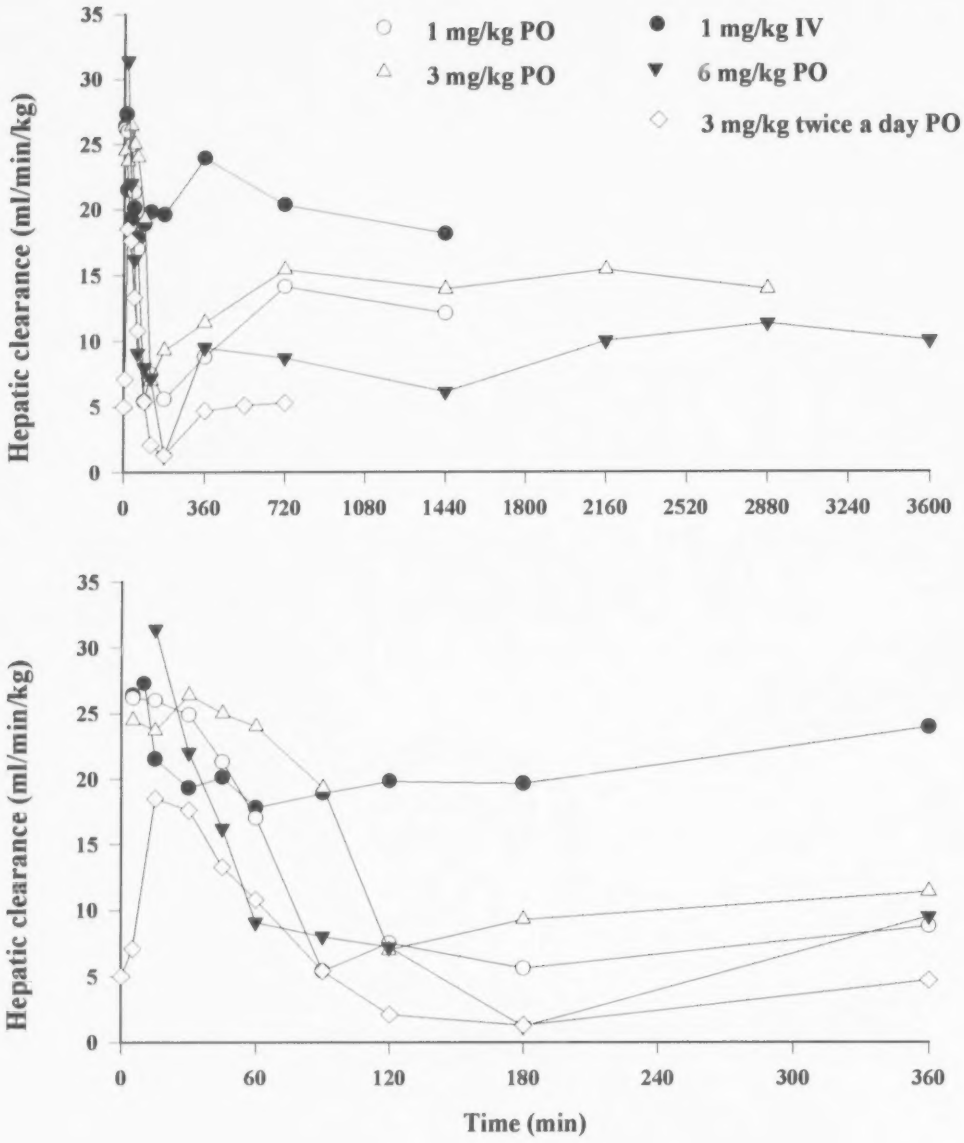

Figure 3.11 Time course of the mean hepatic clearance after 1 mg/kg intravenous and oral administration of 1, 3 and 6 mg/kg single and 3 mg/kg multiple oral doses in four dogs. Upper panel comprises the entire time course of the drug in the body, lower panel represents the first 360 min time profile. (For clarity, only mean values are depicted.)

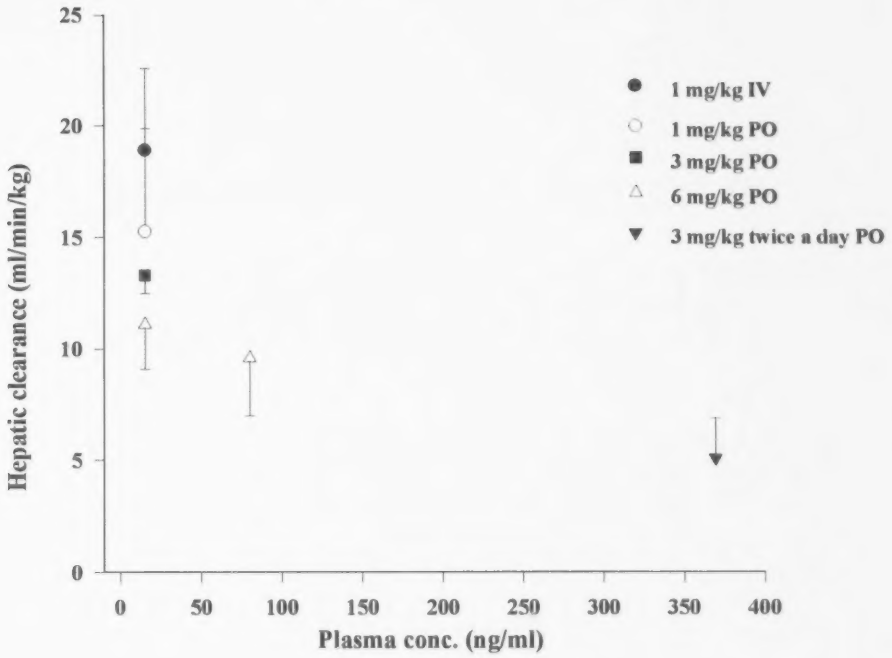

Figure 3.12 Plot of mean hepatic clearance vs. mibefradil plasma concentration in post-absorption, post-distribution phase. Hepatic clearance values were obtained at 15ng/ml mibefradil plasma concentration, after 1mg/kg intravenous and 1, 3 and 6mg/kg single oral doses. Hepatic clearance value at 80ng/ml is shown for 6mg/kg oral dose and for multiple doses at 370ng/ml. Each data point represents an average value from four dogs. Hepatic clearance after 3 and 6mg/kg single and 3mg/kg multiple oral doses was significantly different from the intravenous treatment ($P<0.05$). Single 1mg/kg dose was different from 6mg/kg oral dose at 15ng/ml ($P<0.05$). Hepatic clearance after multiple doses was different from all but 6mg/kg oral dose ($P<0.05$).

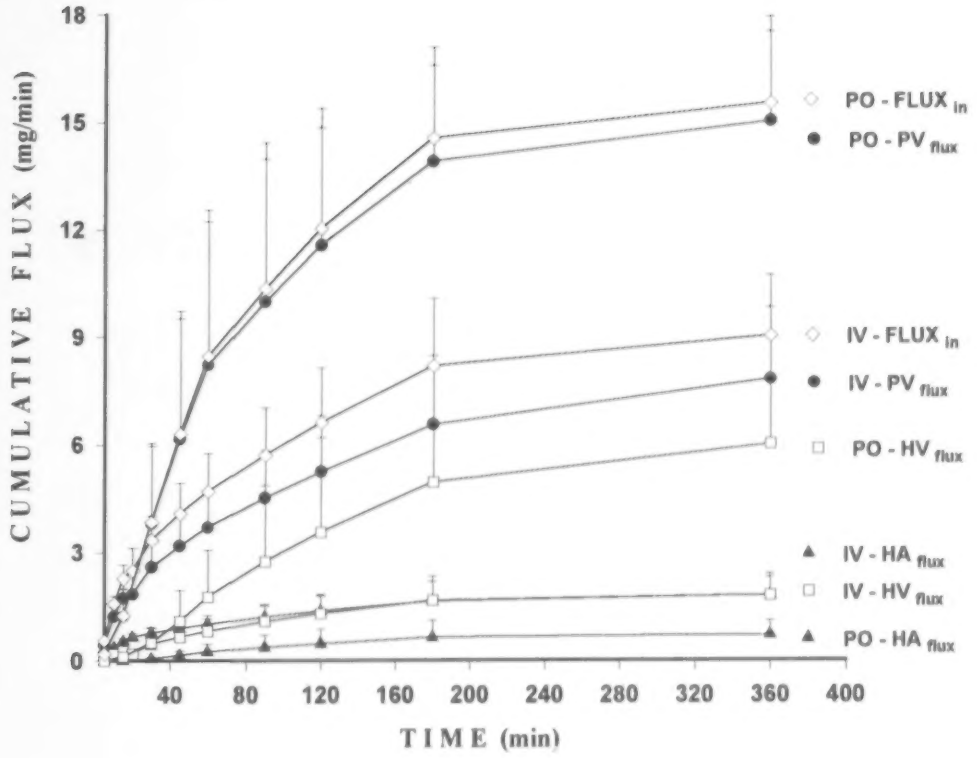

Figure 3.13 Cumulative exposure of the liver to mibefradil after 1 mg/kg intravenous and oral dose to four dogs.

4. DISCUSSION

4.1 HPLC Assay of Mibefradil in Dog Plasma and Urine

The method presently described proved to be selective, sensitive and simple. The assay has been applied successfully to several hundreds of samples from our dog studies. Currently, little information is available on the metabolism of mibefradil in dogs. Metabolism in rats has been intensively investigated (*Wiltshire et al. 1992*) and appears to be complex, giving rise to a multitude of products. Major metabolic pathways include *N*-demethylation, hydrolysis of the ester side chain, hydroxylation, aromatization of the tetrahydronaphthyl system, loss of benzimidazole and glucuronidation of hydroxyl groups. The resultant metabolites are predominantly excreted into the bile. It is reasonable to expect similar metabolic reactions to occur in dogs. Although the extent of biliary excretion of metabolites in dogs is unknown, our results show that unknown peaks elute before the mibefradil and the internal standard (Fig. 3.1 and 3.2) which could be attributed to the polar metabolites of mibefradil. These unknown peaks do not interfere with quantification of mibefradil in plasma and urine.

4.2 Blood Flow Measurements and Indocyanine Green Kinetics

We have developed a conscious dog preparation in which the rate of drug removal can be measured directly across the liver chronically. This model has proven to be a useful method to study transhepatic insulin balance in normal and pancreatic islet cell-

transplanted dogs (*O'Brien et al. 1990a*; *O'Brien et al. 1990b*) and the interactions between food and drugs that undergo extensive first pass metabolism (*Semple et al. 1990*). In the present study we examined the disposition characteristics of ICG, which is used as a noninvasive marker of liver blood flow and as a test of hepatic function in humans and animals. We monitored ICG plasma time course in systemic circulation and extraction across the liver without subjecting the dog to an anesthetic agent, thus maintaining an experimentally "clean" system. Indeed, several studies demonstrated that sodium pentobarbital (*Vogin et al. 1965*) and halothane (*Fujita et al. 1991*) interfered with liver cell ability to absorb and excrete the dye in experimental dogs receiving these anesthetic agents.

We showed that complex surgical instrumentation did not compromise liver function in our experimental dogs as indicated by the unaltered ICG disposition parameters after surgery (Table 3.2). Moreover, results from liver chemistry tests, before and after instrumentation, remained stable and were within normal limits throughout the course of investigation.

Studies in instrumented dogs showed that ICG has a low systemic blood clearance and this observation is consistent with the low liver extraction measured across the liver. Therefore, the assumption that ICG systemic clearance reflects hepatic blood flow in dogs is invalid. Moreover, dog has one of the lowest dye extraction abilities among animal species studied so far; extraction ratios in rats (*Daemen et al. 1989*) and cats (*Burczynski et al. 1987*) were reported to be 0.30 and 0.26, respectively. Extractions close to 100% have never been observed. In human, an extraction ratio of 0.6-0.8 was measured (*Caesar*

et al. 1961; *Leevy et al. 1962*), but its application in clinical research has been seriously questioned by several investigators (*Skak & Keiding, 1987*; *Bauer et al. 1989*). Our dog data are consistent with the data reported by others (*Banaszak et al. 1960*); however the fact that ICG has a low extraction ratio did not stop researchers from using it to monitor liver hemodynamics in dogs (*Belpaire et al. 1989)*.

The accuracy of the electronically measured hepatic blood flow is of prime importance in this model. Every set of flow probes was factory calibrated and tested for required accuracy. Our own calibrations were consistent with manufacturer's data. Moreover, the accuracy of *in vivo* flow measurements has been verified in sheep using a microsphere technique (*Barnes et al. 1983*). Direct *in-situ* calibration of flow probes has been performed in lactating cattle (*Gorewit et al. 1989*); the transit time ultrasonic flow meter provided accurate measurements of mammary arterial blood flow. Therefore, we have sufficient evidence to support that this method provides an accurate and reliable system for chronic measurements of hepatic blood flow in dogs.

ICG based blood flow consistently overestimated electronically measured hepatic blood flow. According to eq. 3.9, systemic blood clearance and liver extraction ratio of ICG are required to calculate the liver blood flow. Since it is assumed that systemic blood clearance is equal to hepatic clearance, it is clear that the presence of a significant extra-hepatic removal route would lead to an overestimation of hepatic blood flow. Furthermore, nonlinear ICG hepatic uptake would give rise to lower extraction ratio than under linear conditions, resulting in overestimated blood flow. Last, but not least, variability of ICG extraction ratio within measured time interval could also contribute to

erroneous estimates. Extraction ratio is likely the most sensitive parameter due to its low value in dogs. Our data show that ICG lung extraction ratio values amount to 40 % of that of the liver's. Considering that lungs receive total cardiac output, lung elimination of ICG is an important disposition process. Interestingly, the kidney was found to be a major organ responsible for extrahepatic uptake of ICG in cats (*Burczynski et al. 1987*), another potential source of overestimation of ICG hepatic blood clearance. An overestimation of ICG hepatic clearance could also be a result of incomplete sample collection. If one allows for longer sampling, the plasma concentration decline can be described by a sum of two exponentials. We extended the sampling time up to 60 minutes in two dogs. Surprisingly, biexponential decline, with the second phase starting at around 30 minutes, was apparent in one dog only; the last phase accounted for 20% of the total AUC. We certainly cannot extrapolate these observations to the remaining five dogs, but in view of kinetic complexities of ICG, we believe that this degree of underestimation is insignificant in the present context and longer sampling times are unwarranted. We minimized the variability due to blood sampling procedure by rapid and simultaneous withdrawal of samples. Results from individual dogs showed that liver extraction varied up to 40%, but there was no obvious trend pointing towards nonlinear uptake and consequently to reduced extraction. It appears that ICG kinetics in dogs precludes accurate determination of hepatic extraction which could lead to erroneous estimation of blood flows. Our results showed that ICG clearance cannot be used to measure hepatic blood flow accurately. Our second objective was to evaluate whether ICG can be used to estimate relative change in hepatic blood flow. Consistent with a low extraction drug, the systemic clearance

remained unchanged when hepatic blood flow was induced with food, whereas electronically measured liver blood flow registered a 30% increase.

In conclusion, ICG is a poor indicator of hepatic blood flow in dogs and its use for this purpose is not recommended. Since ICG failed to provide accurate measurements of hepatic blood flow, our electronic measurements relied upon the literature validation (*Barnes et al. 1983*, *Gorewit et al. 1989*) and our *in vitro* calibration. However, pharmacokinetic studies with mibefradil showed that systemic and hepatic clearance values are very close[2], suggesting that our dog model provides accurate and reliable hepatic blood flow measurements.

4.3 Mibefradil Pharmacokinetics in Noninstrumented Dogs

In the present study, we evaluated the disposition parameters of mibefradil in the dog in order to assess its suitability as a model for studying the mechanisms of nonlinear pharmacokinetics.

Close examination of the human (*Welker et al. 1989*) and our dog pharmacokinetic data revealed that there are numerous similarities but also differences in the pharmacokinetic characteristics among the two species. Results of intravenous experiments indicate that the distribution of mibefradil in dogs and humans is extensive. The volume of distribution at steady state in dogs and humans is 9.7±3.8 l/kg and 2.6 (1.3-3.5) l/kg, respectively. More than three-fold difference in volume of distribution between

[2] Liver is the main component of mibefradil systemic clearance (see section 4.4, p.84, paragraph 1)

the two species is accompanied by almost three-fold difference in plasma protein binding. It has been found that the binding of mibefradil in dog and human plasma is high with a free fraction of 1% and 0.35%, respectively (*Brand & Meyer, 1988*) The value in dogs was also confirmed in a preliminary study conducted in our laboratory (1.06%) and the value agreed well with that reported in the literature. Elimination characteristics appear to be quite different between the two species. Systemic plasma clearance values of mibefradil in dogs are considerably higher than that of humans, amounting to almost five-fold difference, i.e. 18.4±1.2 ml/min/kg vs. 3.9 (3.1-4.7) ml/min/kg, respectively. It is possible, that higher plasma clearance values of mibefradil in dogs are a result of differences in renal excretion, metabolism and liver blood flow. In our dog study, a negligible amount of intact drug was renally excreted, suggesting that the renal component of systemic plasma clearance was minimal. A similar finding has been reported in humans (*Welker et al. 1989*). A lack of arterio-venous difference between carotid artery and jugular vein mibefradil concentrations in dogs suggests that the lung is an unlikely eliminating organ for this drug. Based on the available data in dogs and humans, it is postulated that the liver may be a major site of mibefradil metabolism and elimination. Using this assumption, mibefradil liver extraction ratios can be estimated using the average hepatic blood flow of 27 ml/min/kg in dogs (*Skerjanec et al. 1994*) and 20 ml/min/kg in humans (*Davies & Morris, 1993*) Values of 0.65 and 0.20 are calculated, suggesting mibefradil has a medium to high extraction ratio in the dog, whereas this drug has a low extraction ratio in humans. This difference in liver extraction can be attributed to higher intrinsic metabolic capacity, higher liver blood flow and lower plasma protein binding in

dogs. A higher liver extraction in conjuction with higher liver blood flow in dogs result in a higher systemic plasma clearance when compared to humans. However, despite the quantitative differences in distribution and elimination between the two species, similar to humans, kinetics in dogs follow a nonlinear pattern after administration of single oral doses, ranging from 1 to 6 mg/kg. This observation is based on a disproportionate increase in AUC_{po} and C_{max} vs. dose. The proportionality between the dose and the AUC of a drug is an important criterion used to determine whether the drug exhibits linear or nonlinear kinetics in the body (*Lin, 1994*). Practically, nonlinear pharmacokinetics are reflected most commonly in a less than or greater than proportional increase in the AUC with an increase in dose (*Ludden, 1991*). Assuming liver is the main determinant of systemic plasma clearance, greater than proportional increase in AUC, as seen in our study (Figure 3.5A), can be attributed to a decrease in elimination and/or an increase in absorption. Many drugs undergo significant presystemic metabolism or degradation in the gut lumen (*Skerjanec et al. 1995*), gut mucosa (*George, 1981*) or the liver (*Pond & Tozer, 1984*). If one or more of these processes is altered (reduced) as the dose increases, greater than proportional increase in AUC with the dose may result (*Wagner, 1985*; *Shand & Rangno, 1972*; *Walle et al. 1978*). Reduction in elimination capacity is often attributed to concentration dependent or Michaelis-Menten type kinetics but others, which are not consistent with the Michaelis-Menten kinetics have also been reported. They are termed as dose and time-dependent processes (*Klotz & Reimann, 1981*; *Klotz et al. 1976*; *Levy, 1986*; *Hussain et al. 1994*; *Saville et al. 1989*). Reduction in elimination could therefore lead not only to higher than predicted accumulation but would also pose a problem in

bioavailability estimation, using the conventional AUC method which is based on the premise that plasma clearance be constant during the elimination of the oral and intravenous doses (*Tozer & Rubin, 1988*). It is therefore difficult to assess the true bioavailability of drugs whose elimination kinetics changes with the route of administration.

Our dog data clearly suggest a trend of dose dependent kinetics of mibefradil after oral administration and the use of dose normalized AUC ratios is not a good estimate of absolute bioavailability. However, the use of this ratio for the lowest oral dose (1 mg/kg) would provide the closest value to the true systemic availability. Assuming complete absorption and constant systemic plasma clearance, bioavailability is estimated to be 0.35 based on the estimated liver extraction. This value would be higher if other organs of elimination contribute to systemic elimination of mibefradil. However, we found an average value of 0.18±0.03 which is lower than what liver extraction can account for. This discrepancy may be due to incomplete drug absorption and/or presystemic intestinal metabolism and similar observations were made in humans (Table 1.1).

The data presented here indicate that the nonlinear pattern is similar between dogs and humans. The results suggest that the absorption through the gut and liver elimination are the two parameters worthwhile studying in greater detail. Detailed experimentation, otherwise inaccessible in humans, would therefore call for an appropriately instrumented animal model. Chronically instrumented, conscious dog model has been established recently in our laboratory (*O'Brien et al. 1991*) and allows us to simultaneously monitor the time course of the drug in carotid artery, jugular, portal and hepatic veins with

continuous measurement of hepatic blood flow. Therefore, the absorption through the gut and the rate of drug removal by the liver can be measured and quantified in a conscious animal. Therefore, the contribution of organs involved in elimination of mibefradil and their role in the nonlinear kinetic behaviour could be studied. The findings from the studies using instrumented dogs will be discussed in the next section.

4.4 Mibefradil Pharmacokinetics in Instrumented Dogs

In this study we examined the characteristics of mibefradil disposition in chronically instrumented dogs after intravenous and oral doses. Our previous study in dogs demonstrated that oral clearance values decreased with increasing oral doses and we postulated that saturable first-pass metabolism and/or reduction in hepatic clearance could be responsible (*Skerjanec et al. 1995*). Unfortunately, the design of that study did not permit quantification of organ involvement in presystemic metabolism and therefore, it was not possible to study the mechanisms of nonlinearity. Chronically instrumented, conscious dog model (*O'Brien et al. 1991*) offers a powerful tool to identify and quantify the parameters responsible for dose-dependent disposition of mibefradil. Due to the observed nonlinearity after single oral doses, we felt that long term oral treatment effect should also be studied. For this purpose, we dosed the animals with 3 mg/kg mibefradil orally every 12h for a period of 8 days.

Intravenous experiments revealed that mibefradil is extensively distributed in the body and has a high systemic clearance value, confirming the observations made in

noninstrumented dogs (Skerjanec *et al.*, 1995). In this study, it has been found that the hepatic clearance values are insignificantly different from systemic clearance, suggesting that liver is the major organ for eliminating mibefradil (Table 3.8). Negligible recovery of mibefradil in urine observed in the previous study (Skerjanec *et al.*, 1995) is consistent with this observation. This set of data also implies that pulmonary elimination of mibefradil in dogs is insignificant.

After oral administration, the dose dependent kinetics of mibefradil could be due to nonlinear absorption and/or elimination. Our results clearly indicate that the dose dependent increase in bioavailability is due to a reduction in hepatic extraction but not due to a dose-dependent increase in gut absorption. Together with a reduction in hepatic extraction and clearance, the AUC values of mibefradil during multiple dosing increased five-fold which is more than expected when single dose parameters were used for calculation (eq. 1.2).

At the present time, it is not clear what the exact mechanisms are for the reduction in hepatic clearance. Michaelis-Menten kinetics are often implicated in the nonlinear liver first-pass metabolism of many drugs (*Ludden, 1991*). In this study, it is doubtful that the observed nonlinear first-pass effect is attributed solely to Michaelis-Menten type kinetics. By examining the time course of hepatic extraction after single oral doses during the first 120 minutes (lower panel, Fig. 3.9), there is evidence that Michaelis-Menten kinetics occur to a limited degree during the absorption and distribution of mibefradil in the body. E_H decreases as the concentration in the portal circulation increases during peak absorption and E_H rebounds to a level which is lower than that observed after intravenous

dose and this level remained stable throughout the study. However, the kinetic characteristics of mibefradil point toward a mixture of concentration dependent and independent elimination. After the observed rebound of E_H, mibefradil hepatic extraction never returned to a level observed after intravenous administration (Fig. 3.9). During this period (upper panel, second phase), E_H values are inversely related to oral dose. The events in the second phase suggest that the kinetics of mibefradil are determined by the extent of previous exposure to the drug, which is the highest during the absorption phase. Interestingly, E_H remains constant in the post-absorption, post-distribution phase which is reflected in a log-linear plasma concentration vs. time profiles (Fig. 3.6, lower panel), suggesting that kinetics become linear in this phase. The lower E_H values when compared to an intravenous dose may be due to inactivation of metabolic enzymes, metabolic product inhibition and/or saturation of tight binding to hepatic tissue sites. Lowest E_H and Cl_H values in terminal disposition phase was observed after multiple dosing, suggesting that the reduction in elimination is not only a dose-dependent but also a time-dependent process. Interestingly, during the absorption phase the concentration dependent processes are preserved since the extraction ratio decreases as the absorption of the drug proceeds but it rebounds after 120 min, when the absorption is almost complete. Unlike after single oral doses, hepatic extraction ratio during multiple dosing returns to its predose level, suggesting that the processes responsible for the observed dose-dependency after single oral doses become saturated, as a result of continuous exposure of the system to the drug. However, continuous exposure results in the lowest E_H and Cl_H values, when compared to the single dose treatment groups. When we examined the relationship between the hepatic

clearance and the mibefradil plasma concentrations in the terminal disposition phase (Fig. 3.12), a four-fold difference in hepatic clearance values between the individual treatments was observed for mibefradil concentrations at 15 ng/ml, obtained after single intravenous and oral doses. This observation is inconsistent with Michaelis-Menten type kinetics, because the clearance at a given drug concentration should be the same whether a high or low dose is given (*Gibaldi, 1984*). Consistent with the dose- and time-dependent kinetics, lowest elimination clearance was observed after multiple doses (Fig. 3.12), but the difference is less dramatic when compared to the 6mg/kg dose, suggesting that either high enough dose or long term exposure of the body to the drug will lead to the saturation of the processes, governing the dose dependent disposition of the drug in the body.

There is some evidence to suggest that saturation of hepatic tissue binding plays an important role because V_β values decrease with increasing dose and with duration of the treatment (Table 3.7). The fact that $t_{½}$ values did not change with increasing single oral doses and did not reflect the extent of reduction in hepatic clearance after 3 mg/kg multiple doses when compared to a 3 mg/kg single dose values, suggest that V_β is directly related to Cl_S. The effect of volume of distribution alteration on clearance has not been explored because it is widely accepted that changes in tissue binding have no effect on clearance (*Gibaldi & McNamara, 1978*; *Wedlund & Wilkinson, 1984*; *Rubin & Tozer, 1986*). This concept may be incorrect if the binding is to liver tissues and provides preferential elimination of drug by liver enzymes. However, it has also been recognized that a change in may not reflect a real change in volume of distribution (*Jusko & Gibaldi, 1972*). This estimate can be biased by a change in elimination; this is especially true for

drugs with rapid elimination, where terminal elimination phase half-life accounts for a small portion of the overall AUC. The study by Jusko & Gibaldi has also shown that the decrease in elimination had little effect on the volume of distribution for drugs with longer half-life (>7h). In our case, the terminal phase accounts for more than 70% of the total AUC, suggesting a reduction in clearance would have little effect on V_β estimation. The fact that half-life was insensitive to changes in hepatic clearance, suggests that the decrease in elimination after higher single and multiple oral doses is accompanied by a decrease in distribution.

A time dependent change in hepatic tissue binding has been recently observed with diltiazem (*Hussain et al. 1994*). Mechanism of dose and time-dependent inactivation of hepatic enzyme(s) is not uncommon and has been observed with drugs such as lidocaine (*Saville et al. 1989*) and verapamil (*Schwartz et al. 1985*). It has been postulated that drugs with a tertiary amino group can inactivate *N*-dealkylating CYP isozymes by forming stable metabolic intermediates (*Bast et al. 1990*). Mibefradil fulfills the structural requirements for such a drug, since its chemical structure contains a tertiary amino group (Fig. 3.7). However, there is no information in our set of data to support or deny the enzyme involvement. Another possible mechanism is product inhibition of drug metabolism which can lead to dose and time-dependent changes in elimination kinetics. It has been found that nordiazepam inhibits the metabolism of diazepam (*Klotz et al. 1976*) and following multiple dosing, leads to a time-dependent reduction of diazepam elimination (*Klotz & Reimann, 1981*). It remains to be determined with forthcoming *in-vitro* studies, which of these mechanisms is responsible.

Although it is quite well-known that F measurements using the AUC ratio method is inaccurate when unequal intravenous and oral doses are used and when nonlinear kinetics are involved, in this study, we found that even when identical intravenous and oral doses are used, F estimation using the AUC ratio method can also be erroneous. The reason is that systemic clearance is dependent upon the cumulative exposure of the liver to the drug, which is higher after oral administration (Fig. 3.13).

At this point we'd like to comment on the methodology used for calculating the pharmacokinetic parameters in this study. As the data showed, pharmacokinetics of mibefradil is nonlinear, when intravenous and oral treatments are compared between each other. The calculations that we used in our data analysis assume linear disposition. However, the parameters such as hepatic extraction and clearance were determined directly using physiological measurements which are not affected by nonlinear processes. Volume of distribution in a terminal disposition phase was calculated with the objective to provide an estimate of distribution events after the absorption and distribution of the drug is complete. These calculations were not affected by nonlinearity because the kinetics in terminal disposition phase appear to be linear within an individual treatment group.

From this study, we conclude that the observed nonlinear kinetics of mibefradil in dogs is mainly due to dose- and time-dependent reductions of hepatic clearance. Presently, the exact cause of this phenomenon is not known. The instrumented dog model is shown to be a powerful tool for the evaluation of organ contribution to nonlinear absorption and clearance. The observed results provide a clear direction for *in vitro*

investigations which involve hepatic tissue binding studies and metabolic and enzymatic profiling of mibefradil.

5. SUMMARY AND CONCLUSIONS

A series of experiments was performed, using the dog as an animal model to study the properties and mechanism(s) of nonlinear pharmacokinetics of mibefradil. Initially, we developped and HPLC assay to separate and quantitate mibefradil in biological samples. By utilizing this assay we studied the disposition of mibefradil in plasma and urine after its administration to dogs.

We began our animal studies with preliminary tests of physiological viability of the model and the performance of hepatic blood flow measurements. We showed that complex surgical instrumentation did not compromise liver function in our experimental dogs as indicated by the unaltered ICG disposition parameters after surgery. However, ICG was a poor indicator of hepatic blood flow in dogs due to its low hepatic extraction. On the contrary, the continuous electronic measurements of hepatic blood flow proved to be accurate and consistent during a long term application in the animal.

Preliminary pharmacokinetic studies in intact animals showed that the characteristics of nonlinear pharmacokinetics of mibefradil are qualitatively similar in dogs and humans. We concluded that the dog is an adequate animal model for further studies of the mechanisms of mibefradil nonlinear pharmacokinetics in humans.

By using the chronically instrumented conscious dog model, the involvement of organs such as gut and liver in nonlinear first-pass effect could be identified and quantified. Due to the nonlinearity after single oral doses, we also examined a long term oral treatment effect upon the pharmacokinetics of mibefradil. In the study with the instrumented dogs, we found that liver is the major organ for eliminating mibefradil. We

postulated (*Skerjanec et al. 1995*) that the dose dependent kinetics of mibefradil could be due to nonlinear absorption and/or elimination. Results showed that the dose dependent increase in bioavailability is due to a reduction in hepatic extraction but not due to a dose-dependent increase in gut absorption. Together with a reduction in hepatic extraction and clearance, the AUC values of mibefradil during multiple dosing increased five-fold compared to a single dose AUC values, which is more than expected when single dose parameters were used for calculation. Reduction in hepatic clearance after oral administration in relation to intravenous kinetics resulted in an overestimation of absolute bioavailability. An important finding was that even when equal intravenous and oral doses were used, the conventional area ratio approach produced inaccurate absolute bioavailability values, because systemic clearance is dependent upon the cumulative exposure of the liver to the drug, which is higher after oral administration.

Our studies showed that dog is a suitable animal model to study the mechanisms of nonlinear pharmacokinetics in humans. Close examination of the human (*Welker et al. 1989*) and our dog pharmacokinetic data revealed that there are numerous similarities but also differences in the pharmacokinetic characteristics among the two species. Elimination characteristics appear to be quite different between the two species. Based on the experiments performed with dogs, liver appears to be a major site of mibefradil metabolism and elimination. Liver also appears to be the main eliminating organ in humans due to negligible urinary excretion of the parent drug, which did not change after a range of intravenous and oral doses. Moreover, kidney metabolism of mibefradil could be ruled out due to the low immunoreactivity for CYP enzymes, observed in this tissue

(*Krishna and Klotz, 1994*). Pulmonary elimination in humans is unlikely in the view of a low systemic clearance. Using this assumption, estimated mibefradil liver extraction ratios in dogs and in humans were 0.65 and 0.20, respectively. However, despite the quantitative differences in elimination between the two species, similar to humans, kinetics in dogs follow a nonlinear pattern after administration of single oral and multiple doses. Studies in dogs showed that the absorption from the gut is incomplete and independent of the dose. Nonlinear kinetics occured solely due to a reduction in liver elimination capacity. Detailed analysis of human data (Table 1.1) suggests that absorption is incomplete and greater than proportional increase in AUC (Fig. 1.2) after oral doses appears to be mainly due to a reduction in liver elimination capacity. Interestingly, hepatic extraction in dogs during the absorption phase is significantly reduced, resulting in hepatic extraction values with a characteristic of a low extracted drugs. In this respect, it seems that quantitative differences in hepatic extraction diminish between the two species as the dose increases and during multiple dosing.

At the present time, the exact mechanisms of the dose- and time-dependent reduction in hepatic clearance are unknown. Dose dependent processes may occur as a result of saturable tight binding to hepatic tissue sites, inactivation of CYP hepatic enzyme(s) and/or metabolic product inhibition. Our *in vivo* experimental data warrant future *in vitro* experiments, involving hepatic tissue binding studies and metabolic and enzymatic profiling of mibefradil.

6. REFERENCES

Amidon, G. L., Merfeld, A. E., and Dressman, J. B. Concentration and pH dependency of alpha-methyldopa absorption in rat intestine. *Journal of Pharmacy & Pharmacology* 38:363-368, 1986.

Anonymous. Effect of verapamil on mortality and major events after acute myocardial infarction (the Danish Verapamil Infarction Trial II--DAVIT II). *American Journal of Cardiology* 66:779-785, 1990.

Banaszak, E. F., Steikel, W. J., Grace, R. A., and Śmith, J. J. Estimation of hepatic blood flow using a single injection dye clearance method. *American Journal of Physiology* 198:977-880, 1960.

Barnes, R. J., Comline, R. S., Dobson, A., and Drost, C. J. An implantable transit time ultrasonic blood flowmeter. *Journal of Physiology* 345:2P-3P, 1983.

Barrett, W. E. and Bianchine, J. R. The bioavailability of ultramicrosize griseofulvin (Gris-PEG) tablets in man. *Current Therapeutic Research, Clinical & Experimental* 18:501-509, 1975.

Bast, A., Valk, A. J., and Timmerman, H. Cytochrome P-450 metabolic-intermediate complex formation with a series of diphenhydramine analogues. *Agents & Actions* 30:161-165, 1990.

Bauer, L. A., Horn, J. R., and Opheim, K. E. Variability of indocyanine green pharmacokinetics in healthy adults. *Clinical Pharmacy* 8:54-55, 1989.

Bean, B. P. Classes of calcium channels in vertebrate cells. [Review]. *Annual Review of Physiology* 51:367-384, 1989.

Becton Dickinson, Indocyanine Green; Package Insert.

Belpaire, F. M., Bourda, A., De Smet, F., Rosseel, M. T. and Bogaert, M. G. Influence of lignocaine on plasma protein binding and pharmacokinetics of verapamil in dogs. *Journal of Pharmacy and Pharmacology* 42:45-49, 1989.

Benham, C. D. and Tsien, R. W. Noradrenaline modulation of calcium channels in single smooth muscle cells from rabbit ear artery. *Journal of Physiology* 404:767-784, 1988.

Bertilsson, L., Hojer, B., Tybring, G., Osterloh, J., and Rane, A. Autoinduction of carbamazepine metabolism in children examined by a stable isotope technique. *Clinical Pharmacology & Therapeutics* 27:83-88, 1980.

Bian, K. and Hermsmeyer, K. Ca^{2+} channel actions of the non-dihydropyridine Ca^{2+} channel antagonist Ro 40-5967 in vascular muscle cells cultured from dog coronary and saphenous arteries. *Naunyn-Schmiedebergs Archives of Pharmacology* 348:191-196, 1993.

Billman, G. E. Effect of calcium channel antagonists on susceptibility to sudden cardiac death: protection from ventricular fibrillation [published erratum appears in J Pharmacol Exp Ther 1990 Dec; 255(3):1407]. *Journal of Pharmacology & Experimental Therapeutics* 248:1334-1342, 1989.

Billman, G. E. Ro 40-5967, a novel calcium channel antagonist, protects against ventricular fibrillation. *European Journal of Pharmacology* 229:179-187, 1992.

Boden, W. E., Krone, R. J., Kleiger, R. E., Oakes, D., Greenberg, H., Dwyer, E. J.,Jr., Abrams, J., Coromilas, J., Goldstein, R., and et al. Electrocardiographic subset analysis of diltiazem administration on long-term outcome after acute myocardial infarction. The

Multicenter Diltiazem Post-Infarction Trial Research Group. *American Journal of Cardiology* 67:335-342, 1991.

Bonasch, H. and Cornelius, C. E. Indocyanine green clearance - a liver function test for the dog. *American Journal of Veterinary Research* 25:254-259, 1964.

Boulanger, C. M., Nakashima, M., Olmos, L., Joly, G., and Vanhoutte, P. M. Effects of the Ca^{2+} antagonist RO 40-5967 on endothelium-dependent responses of isolated arteries. *Journal of Cardiovascular Pharmacology* 23:869-876, 1994.

Brand, R. and Meyer, J. In vitro protein binding of the new Ca-antagonist Ro 40-5967 in the plasma of several animal species and man (Exploratory study). *Roche Research Report No. B-104'194*, 1988.

Braunwald, E. Mechanism of action of calcium-channel blocking agents. *New England Journal of Medicine* 307:1618-1627, 1982.

Burczynski, F. J., Pushka, K. L., Sitar, D. S., and Greenway, C. V. Hepatic plasma flow: accuracy of estimation from bolus injections of indocyanine green. *American Journal of Physiology* 252:H953-62, 1987.

Caesar, J., Sheldon, S., Chiandussi, L., Guevara, L., and Sherlock, S. The use of indocyanine in the measurements of hepatic blood flow and as a test of hepatic function. *Clinical Sciences* 21:43-57, 1961.

Carmeliet, E. The slow inward current: nonvoltage-clamp studies. In: *The slow inward current and cardiac arrhythmias*, edited by D. P. Zipes, J. C. Baile and V. Elharrar. Boston: Martinus Nijhoff, 1980, p. 97-110.

Carmeliet, E. Role of calcium channels in cardiac arrhythmias. In: *The calcium channel: structure, function and implications*, edited by M. Morad, W. Nayles, S. Kazda and M. Scramm. Springer Verlag: Martinus Nijhoff, 1988, p. 311-316.

Catterall, W. A., Seagar, M. J., Takahashi, M., and Nunoki, K. Molecular properties of voltage-sensitive calcium channels. [Review]. *Advances in Experimental Medicine & Biology* 255:101-109, 1989.

Chen, I. W., Dorley, J. M., Ramjit, H. G., Pitzenberger, S. M., and Lin, J. H. Physiological disposition and metabolism of L-365,260, a potent antagonist of brain cholecystokinin receptor, in laboratory animals. *Drug Metabolism & Disposition* 20:390-395, 1992.

Chungi, V. S., Bourne, D. W. A., and Dittert, L. W. Drug absorption VIII. Kinetics of GI absorption of methotrexate. *Journal of Pharmaceutical Sciences* 67:560-561, 1978.

Clozel, J. P., Banken, L., and Osterrieder, W. Effects of Ro 40-5967, a novel calcium antagonist, on myocardial function during ischemia induced by lowering coronary perfusion pressure in dogs: comparison with verapamil. *Journal of Cardiovascular Pharmacology* 14:713-721, 1989.

Clozel, J. P. and Kleinbloesem, C. Chemistry and Technical Data. *Roche Report B-106'477*, 1989.

Clozel, J. P., Veniant, M., and Osterrieder, W. The structurally novel Ca2+ channel blocker Ro 40-5967, which binds to the [3H] desmethoxyverapamil receptor, is devoid of the negative inotropic effects of verapamil in normal and failing rat hearts. *Cardiovascular Drugs & Therapy* 4:731-736, 1990.

Daemen, M. J., Thijssen, H. H., van Essen, H., Vervoort-Peters, H. T., Prinzen, F. W. S.,Boudier HA, and Smits, J. F. Liver blood flow measurement in the rat. The electromagnetic versus the microsphere and the clearance methods. *Journal of Pharmacological Methods* 21:287-297, 1989.

Daneshmend, T. K., Jackson, L., and Roberts, C. J. C. Physiological and pharmacological variability in estimated hepatic blood flow in man. *British Journal of Clinival Pharmacology* 11: 491-496, 1981.

Davies, B. and Morris, T. Physiological parameters in laboratory animals and humans. [Review]. *Pharmaceutical Research* 10:1093-1095, 1993.

Doi, R., Inoue, K., Kogire, M., Sumi, S., Takaori, K., Suzuki, T., and Tobe, T. Simultaneous measurement of hepatic arterial and portal venous flows by transit time ultrasonic volume flowmetry. *Surgery, Gynecology & Obstetrics* 167:65-69, 1988.

Dressman, J. B. and Fleisher, D. Mixing-tank model for predicting dissolution rate control or oral absorption. *Journal of Pharmaceutical Sciences* 75:109-116, 1986.

Dressman, J. B., Fleisher, D., and Amidon, G. L. Physicochemical model for dose-dependent drug absorption. *Journal of Pharmaceutical Sciences* 73:1274-1279, 1984.

Dromgoole, S. H. and Furst, D. E. Salicylates. In: *Applied pharmacokinetics: principles of therapeutic drug monitoring*, edited by W. E. Evans, J. J. Schentag and W. J. Jusko. Vancouver, WA: Applied Therapeutics, Inc. 1992, p. 32-1 - 32-34.

Echizen, H. and Eichelbaum, M. Clinical pharmacokinetics of verapamil, nifedipine and diltiazem. [Review]. *Clinical Pharmacokinetics* 11:425-449, 1986.

Ezzaher, A., el Houda Bouanani, N., Su, J. B., Hittinger, L., and Crozatier, B. Increased negative inotropic effect of calcium-channel blockers in hypertrophied and failing rabbit heart. *Journal of Pharmacology & Experimental Therapeutics* 257:466-471, 1991.

Fang, L. M. and Osterrieder, W. Potential-dependent inhibition of cardiac Ca^{2+} inward currents by Ro 40-5967 and verapamil: relation to negative inotropy. *European Journal of Pharmacology* 196:205-207, 1991.

Fleckenstein, A. Specific pharmacology of calcium in myocardium, cardiac pacemakers, and vascular smooth muscle. [Review]. *Annual Review of Pharmacology & Toxicology* 17:149-166, 1977.

Fox, A. P., Nowycky, M. C., and Tsien, R. W. Kinetic and pharmacological properties distinguishing three types of calcium currents in chick sensory neurones. *Journal of Physiology* 394:149-172, 1987.

Fozzard, H. A. Calcium Channels in the heart. In: *Calcium antagonists - the state of the art and role in cardiovascular disease*, edited by B. F. Hoffman. Philadelphia: College of Physicians of Philadelphia, 1983, p. 7-12.

Fujita, Y., Kimura, K., Hamada, H., and Takaori, M. Comparative effects of halothane, isoflurane, and sevoflurane on the liver with hepatic artery ligation in the beagle. *Anesthesiology* 75:313-318, 1991.

Gasser, R., Hauri, H. P., and Meyer, U. A. The turnover of cytochrome P450b. *FEBS Letters* 147:239-242, 1982.

George, C. F. Drug metabolism by the gastrointestinal mucosa. *Clinical Pharmacokinetics* 6:259-274, 1981.

Gibaldi, M. *Biopharmaceutics and Clinical Pharmacokinetics.* Philadelphia: Lea & Febiger, 1984. p.197.-200.

Gibaldi, M. and McNamara, P. J. Apparent volumes of distribution and drug binding to plasma proteins and tissues. *European Journal of Clinical Pharmacology* 13:373-380, 1978.

Gibaldi, M. and Perrier, D. *Pharmacokinetics.* New York: Marcel Dekker, 1982. p.409-416.

Godfraind, T., Morel, N., and Wibo, M. Tissue specificity of dihydropyridine-type calcium antagonists in human isolated tissues. [Review]. *Trends in Pharmacological Sciences* 9:37-39, 1988.

Gorewit, R. C., Aromando, M. C., and Bristol, D. G. Measuring bovine mammary gland blood flow using a transit time ultrasonic flow probe. *Journal of Dairy Science* 72:1918-1928, 1989.

Gray, G. A., Clozel, M., Clozel, J. P., and Baumgartner, H. R. Effects of calcium channel blockade on the aortic intima in spontaneously hypertensive rats. *Hypertension* 22:569-576, 1993.

Guth, B. D. Reduction of exercise-induced regional contractile dysfunction in dogs using a novel calcium channel blocker (Ro 40-5967). *Cardiovascular Drugs & Therapy* 6:167-171, 1992.

Hagiwara, S. and Byerly, L. Calcium channel. [Review]. *Annual Review of Neuroscience* 4:69-125, 1981.

Hefti, F., Clozel, J. P., and Osterrieder, W. Antihypertensive properties of the novel calcium antagonist (1S,2S)-2-[2-[[3-(2-benzimidazolyl)propyl]methylamino]ethyl]-6-fluoro-1,2,3,4-tetrahydro-1-isopropyl-2-naphthyl methoxyacetate dihydrochloride in rat models of hypertension. Comparison with verapamil. *Arzneimittel-Forschung* 40:417-421, 1990.

Heintz, R., Svensson, C. K., Stoeckel, K., Powers, G. J. and Lalka, D. Indocyanine Green: pharmacokinetics in the rabbit and relevant studies of its stability and purity. *Journal of Pharmaceutical Sciences* 75:398-402, 1986.

Hermann, P. and Morselli, P. L. Pharmacokinetics of diltiazem and other calcium entry blockers. [Review]. *Acta Pharmacologica et Toxicologica* 57 Suppl 2:10-20, 1985.

Hermsmeyer, K. Differences of calcium channels in vascular muscle in hypertension. *American Journal of Hypertension* 4:412S-415S, 1991.

Hoglund, P. and Nilsson, L. G. Pharmacokinetics of diltiazem and its metabolites after single and multiple dosing in healthy volunteers. *Therapeutic Drug Monitoring* 11:558-566, 1989.

Hosey, M. M., Chang, F. C., O'Callahan, C. M., and Ptasienski, J. L-type calcium channels in cardiac and skeletal muscle. Purification and phosphorylation. [Review]. *Annals of the New York Academy of Sciences* 560:27-38, 1989.

Hussain, M. D., Tam, Y. K., Gray, M. R., and Coutts, R. T. Mechanisms of time-dependent kinetics of diltiazem in the isolated perfused rat liver. *Drug Metabolism & Disposition* 22:36-42, 1994.

Jusko, W. J. and Gibaldi, M. Effects of change in elimination on various parameters of the two-compartment open model. *Journal of Pharmaceutical Sciences* 61:1270-1273, 1972

Kihara, Y. and Morgan, J. P. Intracellular calcium and ventricular fibrillation. Studies in the aequorin-loaded isovolumic ferret heart. *Circulation Research* 68:1378-1389, 1991.

Klotz, U., Antonin, K. H., and Bieck, P. R. Comparison of the pharmacokinetics of diazepam after single and subchronic doses. *European Journal of Clinical Pharmacology* 10:121-126, 1976.

Klotz, U. and Reimann, I. Clearance of diazepam can be impaired by its major metabolite desmethyldiazepam. *European Journal of Clinical Pharmacology* 21:161-163, 1981.

Kraft, W., Lechner, J., Vollmar, A. M., Reusch, C., Warmbier, M., and Lohss, E. [Indocyanine green test in the dog]. [German]. *Tierarztliche Praxis* 19:439-446, 1991.

Krishna, D. R. and Klotz, U. Extrahepatic metabolism of drugs in humans. *Clinical Pharmacokinetics* 26:144-160, 1994.

Leevy, C. M., Mendenhall, C. H., Lesko, W., and Howard, M. J. Estimation of hepatic blood flow with indocyanine green. *Journal of Clinical Investigation* 41:1169-1179, 1962.

Levy, G. and Gibaldi, M. Pharmacokinetics. In: *Concepts in Biochemical Pharmacology: Handbook for Experimental Pharmacology*, edited by J. R. Gillette and J. R. Mitchell. New York: Springer, 1975, p. 1-34.

Levy, M. N. Role of calcium in arrhythmogenesis. [Review]. *Circulation* 80:IV23-30, 1989.

Levy, R. H. Time-dependent Pharmacokinetics. In: *Pharmacokinetics: Theory and Methodology*, edited by M. Rowland and G. Tucker. Pergamon Press, 1986, p. 115-129.

Lin, J. H. Dose-dependent pharmacokinetics: experimental observations and theoretical considerations. [Review]. *Biop.armaceutics & Drug Disposition* 15:1-31, 1994.

Ludden, T. M. Nonlinear pharmacokinetics: clinical Implications. [Review]. *Clinical Pharmacokinetics* 20:429-446, 1991.

Lüscher, T. F. and Vanhoutte, P. M. *The endothelium: modulator of cardiovascular function.* Boca-Raton: CRC Press, 1990. p.1-228.

Merillat, J. C., Lakatta, E. G., Hano, O., and Guarnieri, T. Role of calcium and the calcium channel in the initiation and maintenance of ventricular fibrillation. *Circulation Research* 67:1115-1123, 1990.

Metzler, C. M. and Weiner, D. L. *PCNONLIN, Ver. 4.1.* Lexington,Kentucky: SCI Software, 1992.

Miller, R. J. Multiple calcium channels and neuronal function. [Review]. *Science* 235:46-52, 1987.

Milliken, G. A. and Johnson, D. E. *Analysis of Messy Data: Designed Experiements.* New York: Van Nostrand Reinhold Company, 1984. p.19-20.

Mishra, S. K. and Hermsmeyer, K. Selective inhibition of T-type Ca^{2+} channels by Ro 40-5967. *Circulation Research* 75:144-148, 1994.

Mishra, S. K. and Hermsmeyer, K. Inhibition of signal Ca^{2+} in dog coronary arterial vascular muscle cells by Ro 40-5967. *Journal of Cardiovascular Pharmacology* 24:1-7, 1994.

O'Brien, D. W., Molnar, G. D., O'Brien, D. C., and Rajotte, R. V. Increased decrease in islet transplanted dogs contributes to peripheral insulinemia. *Diabetologia* 33:A180,1990a.

O'Brien, D. W., Molnar, G. D., Semple, H. A., and O'Brien, D. C. Qauntitatively normal, but quantitatively increased portal insulin secretion in pancreatic islet auto transplanted conscious dogs. *Diabetes* 39:311A,1990b.

O'Brien, D. W., Semple, H. A., Molnar, G. D., Tam, Y., Coutts, R. T., and Rajotte, R. V. BS.,J. A chronic conscious dog model for direct transhepatic studies in normal and pancreatic islet cell transplanted dogs. *Journal of Pharmacological Methods* 25:157-170, 1991.

Opie, L. H. *Drugs for the heart.* W.B.Saunders Company, 1991. p.42.-73.

Oppenheim, A. V. and Schafer, R. W. *Digital Signal Processing.* Englewood Clifs: Prentice Hall, 1975.

Orito, K., Satoh, K., and Taira, N. Cardiovascular profile of Ro 40-5967, a new nondihydropyridine calcium antagonist, delineated in isolated, blood-perfused dog hearts. *Journal of Cardiovascular Pharmacology* 22:293-299, 1993.

Osterrieder, W. and Holck, M. In vitro pharmacologic profile of Ro 40-5967, a novel Ca^{2+} channel blocker with potent vasodilator but weak inotropic action. *Journal of Cardiovascular Pharmacology* 13:754-759, 1989.

Ott, P., Keiding, S. and Bass, L. Plasma elimination of indocyanine green in the intact pig after bolus injection and during constant infusion: comparison of spectrophotometry and high-pressure liquid chromatography for concentration analysis. *Hepatology* 18:1504-1515, 1993.

Pond, S. M. and Tozer, T. N. First-pass elimination: basic concepts and clinical consequences. *Clinical Pharmacokinetics* 9:1-25, 1984.

Rappaport, P. L. and Thiessen, J. J. High-pressure liquid chromatographic analysis of indocyanine green. *Journal of Pharmaceutical Sciences* 71:157-161, 1982.

Reilly, P. A., Inaba, T., Kadar, D., and Endrenyi, L. Enzyme induction following a single dose of amobarbital in dogs. *Journal of Pharmacokinetics & Biopharmaceutics* 6:305-313, 1978.

Rocci, M. L.,Jr. and Jusko, W. J. LAGRAN program for area and moments in pharmacokinetic analysis. *Computer Programs in Biomedicine* 16:203-216, 1983.

Rubin, G. M. and Tozer, T. N. Hepatic binding and Michaelis-Menten metabolism of drugs. *Journal of Pharmaceutical Sciences* 75:660-663, 1986.

SAS for Windows, Release 6.03. *SAS Institute, Inc.*, Cary, NC, 1994.

Saville, B. A., Gray, M. R., and Tam, Y. K. Evidence for lidocaine-induced enzyme inactivation. *Journal of Pharmaceutical Sciences* 78:1003-1008, 1989.

Schmitt, R., Kleinbloesem, C. H., Belz, G. G., Schroeter, V., Feifel, U., PozenelH, Kirch, W., Halabi, A., Woittiez, A. J., Welker, H. A., and et al. Hemodynamic and humoral

effects of the novel calcium antagonist Ro 40-5967 in patients with hypertension. *Clinical Pharmacology & Therapeutics* 52:314-323, 1992.

Schneider, J. A. and Sperelakis, N. Slow Ca^{2+} and Na^{+} responses induced by isoproterenol and methylxantines in isolated perfused guinea-pig hearts exposed to elevated K^{+}. *Journal of Molecular and Cellular Cardiology* 7:249-273, 1975.

Schneider, M. F. and Chandler, W. K. Voltage dependent charge movement of skeletal muscle: a possible step in excitation-contraction coupling. *Nature* 242:244-246, 1973.

Schwartz, J. B., Abernethy, D. R., Taylor, A. A., and Mitchell, J. R. An investigation of the cause of accumulation of verapamil during regular dosing in patients. *British Journal of Clinical Pharmacology* 19:512-516, 1985.

Semple, H. A., Tam, Y. K., and O'Brien, D. W. Physiological modelling of the hepatic interaction between food and hydralazine in the conscious dog. *Pharmaceutical Research* 7:S223,1990.

Shand, D. G. and Rangno, R. E. The disposition of propranolol. I. Elimination during oral absorption in man. *Pharmacology* 7:159-168, 1972.

Sheiner, L. B. and Ludden, T. M. Population pharmacokinetics/dynamics. [Review]. *Annual Review of Pharmacology & Toxicology* 32:185-209, 1992.

Skak, C. and Keiding, S. Methodological problems in the use of indocyanine green to estimate hepatic blood flow and ICG clearance in man. *Liver* 7:155-162, 1987.

Skerjanec, A., Campbell, N. R. C., Robertson, S., and Tam, Y. K. Pharmacokinetics and presystemic gut metabolism of methyldopa in healthy human subjects. *Journal of Clinical Pharmacology* 35:275-280, 1995.

Skerjanec, A., O'Brien, D. W., and Tam, Y. K. Hepatic blood flow measurements and indocyanine green kinetics in a chronic dog model. *Pharmaceutical Research* 11:1511-1515, 1994.

Skerjanec, A. and Tam, Y. K. HPLC analysis of mibefradil in dog plasma and urine. *Journal of Chromatography:Biomedial Applications* 1995, in press

Skerjanec, A., Tawfik, S., and Tam, Y. K. Nonlinear pharmacokinetics of mibefradil: an evaluation of the dog as an animal model. *Journal of Pharmaceutical Sciences*, submitted

SPSS for Windows, Release 6.1. *SPSS, Inc.*, Chicago, IL, 1994.

Tozer, T. N. and Rubin, G. M. Saturable Kinetics and Bioavailability Determination. In: *Pharmacokinetics: Regulatory, Industrial, Academic Perspectives*, edited by P. G. Welling and F. L. S. Tse. New York: Marcel Dekker, Inc. 1988, p. 478-479.

Tozer, T. N. and Winter, M. E. Phenytoin. In: *Applied Pharmacokinetics: Principles of Therapeutic Drug Monitoring*, edited by W. E. Evans, J. J. Schentag and W. J. Jusko. Vancouver, WA: Applied Therapeutics, Inc. 1992, p. 25-1 - 25-44.

Transonic Systems. *Publication Reprint List, 34 Dutch Mill Road, Ithaca NY,* 1992.

Triggle, D. J. Calcium Antagonists. In: *Cardiovascular Pharmacology*, edited by M. J. Antonaccio. New York: Raven Press, 1990, p. 107-160.

Triggle, D. J. Molecular pharmacology of voltage-gated calcium channels. [Review]. *Annals of the New York Academy of Sciences* 747:267-281, 1994.

Tsien, R. W., Lipscombe, D., Madison, D. V., Bley, K. R., and Fox, A. P. Multiple types of neuronal calcium channels and their selective modulation. [Review]. *Trends in Neurosciences* 11:431-438, 1988.

Vander Heide, R. S., Schwartz, L. M., and Reimer, K. A. The novel calcium antagonist Ro 40-5967 limits myocardial infarct size in the dog. *Cardiovascular Research* 28:1526-1532, 1994.

Veniant, M., Clozel, J. P., Hess, P., and Wolfgang, R. Ro 40-5967, in contrast to diltiazem, does not reduce left ventricular contractility in rats with chronic myocardial infarction. *Journal of Cardiovascular Pharmacology* 17:277-284, 1991.

Vogin, E. E., Scott, W., Boyd, J., and Mattis, P. A. Effect of pentobarbital anesthesia on plasma half-life of indocyanine green in beagles. *Proceedings of Society for Experimental Biology and Medicine* 121:1045-1046, 1965.

Wagner, J. A., Guggino, S. E., Reynolds, I. J., Snowman, A. M., Biswas, A., and Olivera, B. M.,Snyder SH. Calcium antagonist receptors. Clinical and physiological relevance. [Review]. *Annals of the New York Academy of Sciences* 522:116-133, 1988.

Wagner, J. G. Propranolol: pooled Michaelis-Menten parameters and the effect of input rate on bioavailability. *Clinical Pharmacology & Therapeutics* 37:481-487, 1985.

Walle, T., Conradi, E. C., Walle, U. K., Fagan, T. C., and Gaffney, T. E. The predictable relationship between plasma levels and dose during chronic propranolol therapy. *Clinical Pharmacology & Therapeutics* 24:668-677, 1978.

Wedlund, P. J. and Wilkinson, G. R. Hepatic tissue binding and the oral first-pass effect. *Journal of Pharmaceutical Sciences* 73:422-425, 1984.

Welker, H. A., Eggers, H., and Kleinbloesem, C. H. Ro 40-5967: pharmacokinetics of a new calcium antagonist. *European Journal of Clinical Pharmacology* 36:A304,1989.

Wilkinson, G. R. and Shand, D. G. A physiological approach to hepatic drug clearance. *Clinical Pharmacology and Therapeutics* 18:377-390, 1975.

Wiltshire, H. R., Harris, S. R., Prior, K. J., Kozlowski, U. M., and Worth, E. Metabolism of calcium antagonist Ro 40-5967: a case history of the use of diode-array u.v. spectroscopy and thermospray-mass spectrometry in the elucidation of a complex metabolic pathway. *Xenobiotica* 22:837-857, 1992.

Wit, A. L. and Cranefield, P. F. Effect of verapamil on the sinoatrial and atrioventricular nodes of the rabbit and the mechanism by which it arrests reentrant atrioventricular nodal tachycardia. *Circulation Research* 35:413-425, 1974.

Zar, J. H. *Biostatistical Analysis.* Englewood Cliffs: Prentice-Hall, 1984. p.228-231.

Zipes, D. P. and Fischer, J. C. Effects of agents which inhibit the slow channel on sinus node automaticity and atrioventricular conduction in the dog. *Circulation Research* 34:184-192, 1974.